# Magmatism in the southeastern Anatolian orogenic belt: transition from arc to post-collisional setting in an evolving orogen

ILKAY KUSCU[1,2]*, GONCA GENCALIOGLU KUSCU[1,2], RICHARD M. TOSDAL[2], THOMAS D. ULRICH[2] & RICHARD FRIEDMAN[2]

[1]*Department of Geological Engineering, Mugla University, TR-48100, Turkey*

[2]*Mineral Deposit Research Unit, Department of Earth and Ocean Sciences, University of British Columbia, V6T 1Z4 Vancouver, BC, Canada*

**Corresponding author (e-mail: ikuscu@eos.ubc.ca; ikuscu@mu.edu.tr)*

**Abstract:** Late Cretaceous to Middle Eocene calc-alkaline to alkaline magmatic rocks emplaced within the southeastern Anatolian orogenic belt, the most extensive magmatic belt in Turkey, result from the complex collision between the Afro-Arabian and Eurasian plates and the subduction of the southern and northern Neotethyan oceanic basins beneath the Eurasian continental margin during the Alpine–Himalayan orogeny. In a transect in east-central Turkey extending from Baskil (Elazig) to Divrigi (Sivas) to the north, and from Copler (Erzincan) to Horozkoy (Nigde) to the SW, these magmatic rocks vary in time, spatial distribution, and composition. $^{40}Ar/^{39}Ar$ ages supplemented by a few U–Pb ages geochronology from major plutons demonstrate a general younging of magmatism in the transect from *c*. 83 Ma in the south (Baskil) to *c*. 69 Ma in the north (Divrigi-Keban), followed by a *c*. 44 Ma scattered magmatic complex now found along a NE trending arcuate belt between Copler and Horoz. In general, trace element and rare earth element (REE) geochemistry in the magmatic rocks suggest two main sources for the melts: (1) a mantle-wedge and subducted oceanic lithosphere producing arc-type magma; and (2) metasomatized lithospheric mantle modified by subduction producing magmatic rocks with more metasomatized mantle and within plate signatures. The combination of geochemical and geochronological data presented herein provides a basis to reconstruct the temporal and spatial transition from subduction-related to post-collision and to late-orogenic magmatism in the eastern Mediterranean region. Subduction-related magmatism is rooted to closure of the Neo-Tethyan Ocean whereas post-collision and late orogenic-within plate-related magmatism is driven by the collision of a northern promontory of the SE Anatolian orogenic belt with northerly derived ophiolitic rocks. The magmatic transition occurs regionally in northerly to northwesterly trending belts in the southeastern Anatolian orogenic belt. The magmatism exhibit a clear shift from deep seated arc-type to late-orogenic from south (Baskil) to more deeply eroded mid-crustal plutons at the north (Divrigi), then to magmatism related to incipient slab-rupture from northeast (Copler, Kabatas, Bizmisen-Calti) to SW (Karamadazi and Horoz). The age progression follows a south-to-north geochemical trend of decreasing crustal input into mantle-derived magmas, and is explained as a consequence of slab roll-back after the collision/obduction of northerly ophiolites followed by slab steepening and incipient rupture leading to transtensional block faulting and subsidence, and thus to the preservation of near-surface magmatic products along a NE trending belt.

Complex earth movements have shaped the Anatolia (Asia Minor) region of Turkey for millions of years. Except for a small part of the country along the Syrian border that is a continuation of the Arabian Platform, Turkey is geologically part of the great Alpine–Himalayan belt, known also as Tethyan collage, which extends from the Atlantic Ocean to the Himalayan Mountains. This belt, which is about 7000 km long, was formed during the Late Cretaceous to Quaternary period, as the Arabian, African, and Indian continental plates began to interact with the Eurasian plate. Caught between colliding continents, the Mesozoic and Cenozoic Tethyan collage stretching from Europe across southern Eurasia is an extremely complex geological terrane. Nonetheless despite the complexity, the geodynamic setting of the Tethyan collage is reasonably well known.

Within the Tethyan collage, the southeastern Anatolian orogenic belt (SEAOB) in east-central Turkey resulted from the closure of former Mesozoic ocean basins, including the incorporation of a number of smaller continental microplates, during the final collision of Arabia with Eurasia. The SEAOB is an arc-shaped orogenic belt (Fig. 1a–c) that extends across Turkey towards western and northwestern Iran (Fig. 1b). In detail, northward subduction of the African–Arabian plate and

*From*: Sosson, M., Kaymakci, N., Stephenson, R. A., Bergerat, F. & Starostenko, V. (eds) *Sedimentary Basin Tectonics from the Black Sea and Caucasus to the Arabian Platform*. Geological Society, London, Special Publications, **340**, 437–460. DOI: 10.1144/SP340.19 0305-8719/10/$15.00 

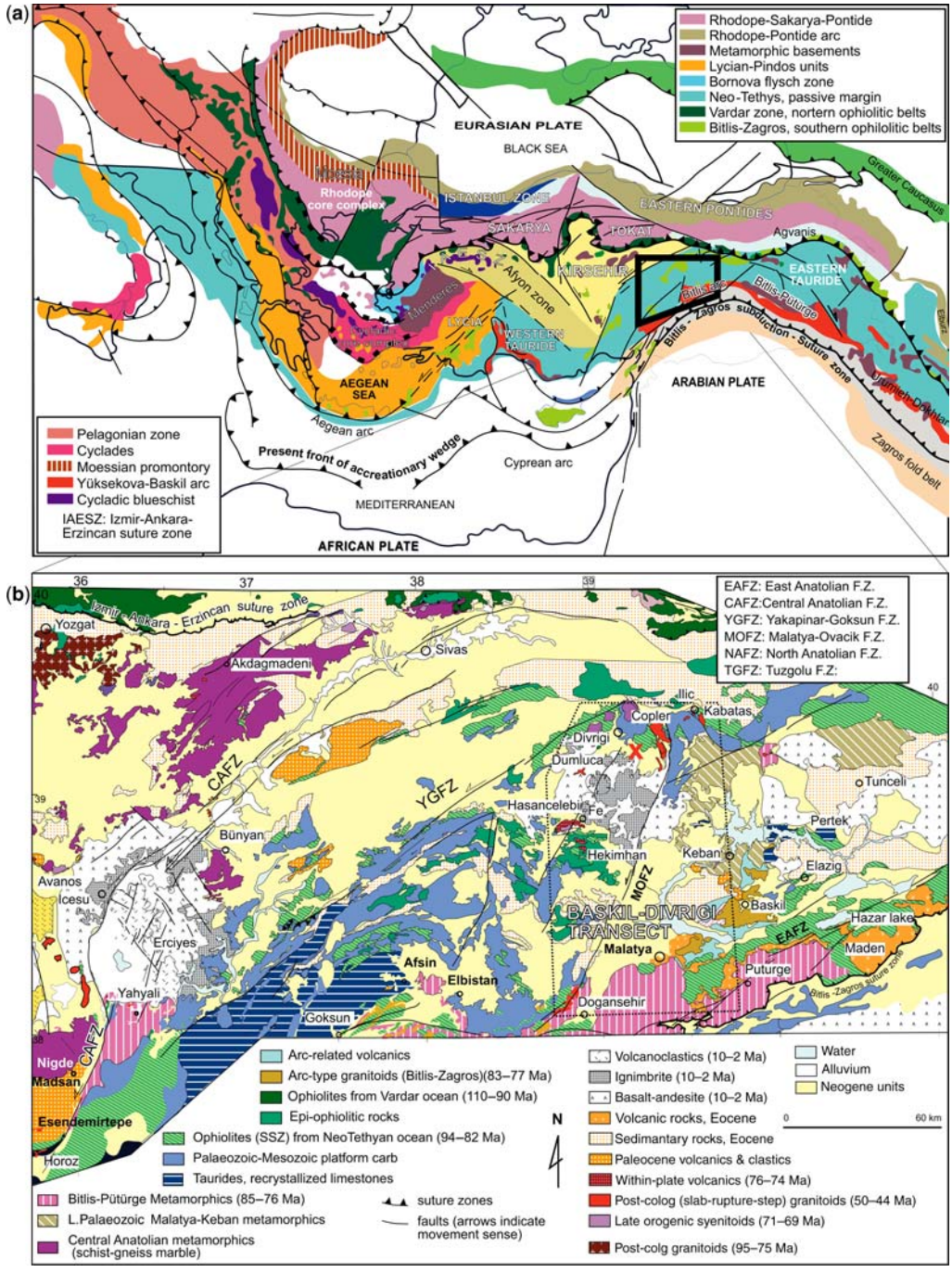


**Fig. 1.** (**a**) Terrane map of Alpine belt showing the correlation of major tectonic units (Modified from http://www-sst.unil.ch/research/plate_tecto/present_day.htm). (**b**) Simplified geological map of eastern Turkey showing the main rock units within the Baskil-Divrigi transect.

related basins of the Neo-Tethys Ocean beneath the Eurasian plate of the eastern Taurides, *sensu stricto*, formed the SEAOB (Aktas & Robertson 1984; Yılmaz 1993; Yılmaz *et al.* 1993; Beyarslan & Bingol 2000; Sengör *et al.* 2003). Subduction initiated during the Late Cretaceous (*c.* 90 Ma) and culminated at the Middle Miocene (Parlak 2005; Robertson *et al.* 2005). Whereas the overall complicated tectonic sequence is reasonably well understood, the magmatic evolution and how these events fit into the tectonic evolution are open to conflicting interpretation. Placing constraints on the magmatic complexes and how they evolve with time and space is the focus of this chapter.

Magmatic processes in rapidly shifting convergent tectonic environments are complicated. In general, the formation of magmas having a subduction-related geochemical signature result from: (1) subduction of oceanic lithosphere (Hawkesworth *et al.* 1993; Pearce & Peate 1995); (2) melting of metasomatically enriched, subcontinental lithosphere with an inherited subduction signature (Turner *et al.* 1996); or (3) extensive crustal contamination of MORB-like (mid-ocean-ridge basalt) magmas (Turner *et al.* 1999). Generation of intraplate-type magmas in continental settings is generally related to upwelling sub-lithospheric mantle material. In Turkey, the subduction-related and late orogenic to within plate-type magmatic rocks are commonly related to kilometre-scale continental extensional terranes. Such a linkage on a global basis is thought to reflect lithospheric response to rapid changes in subduction geometry or reorganization of upper mantle (Bird 1979; Turner *et al.* 1996, 1999; Duggen *et al.* 2003, 2005). Large-scale reorganization of the upper mantle may be related to: (1) roll-back and detachment of subducted oceanic lithosphere (Innocenti *et al.* 1982; Keller 1982; Davies & Blanckenburg 1995; Wilson & Bianchini 1999; Wortel & Spakman 2000); (2) detachment or convective thinning of subcontinental lithosphere (Pearce *et al.* 1990; Platt & England 1993; Turner *et al.* 1999; Lopez-Ruiz *et al.* 2002); or (3) delamination (peeling-off) of subcontinental lithosphere (Bird 1979; Serri *et al.* 1993; Duggen *et al.* 2003).

The processes responsible for uplift and the generation of volcanic areas with geochemically diverse subduction-related and post-collisional to late orogenic-type igneous rocks are still a matter of debate, and poorly understood. As the SEAOB preserves a temporal and spatial transition from convergent margin arc to late-to-post orogenic magmatic events followed by successive extensional periods, it presents a challenge to better constrain the temporal and spatial associations of diverse magmatic events. We address this challenge through a combination of systematic geochemical and geochronological data across a transect between Baskil and Divrigi, which lies normal to the northerly to northwesterly trending magmatic belts within the complex arcute belt lying parallel to the main trend of Bitlis suture zone (Fig. 1c). The data permits the construction of the temporal and spatial framework to place the transition from post-collisional subduction related to late-orogenic magmatism in this eastern Mediterranean region. We summarize herein the magmatic associations based on field criteria, their geochemical compositions supported by the age of magmatism. Our goal is to reconstruct the geological evolution of the Late Cretaceous to Middle Eocene in the Baskil-Divrigi transect, and to identify the temporal and spatial associations of the magmatic events. The transect includes ophiolites originating in the Vardar and Neo-Tethyan Oceans, as well as several calc-alkaline and alkaline magmatic belts including Baskil (Baskil magmatics), Keban (Keban syenite, Elazig), Hasancelebi (Hasancelebi volcanics and syenitoids, Malatya), Divrigi (Murmano pluton, Sivas) Copler-Yakuplu (Copler, Kabatas, Yakuplu pluton, Erzincan) and Bizmisen, Calti (Bizmisen-Calti plutons, Sivas) (Fig. 1) regions. Although, they are not included in the Baskil-Divrigi transect post-collisional magmatic rocks in Karamadazi (Karamadazi granitoid, Kayseri) and Horozkoy (Horoz granite, Nigde) were also evaluated for complementary to spatial and temporal associations related to Late Cretaceous to Eocene events in Bitlis–Zagros subduction zone. The new geochemical and geochronological data presented herein for igneous rocks from this transect in southeastern Turkey are also integrated into a tectonic model.

## Regional tectonic evolution and geodynamic setting

The SEAOB, a microcontinent rifted from Gondwanaland during Early Mesozoic time (Sengör & Yılmaz 1981; Robertson & Woodcock 1982), contains the remains of a Neo-Tethyan Ocean basin that was closed and consumed by a northward subduction beneath the eastern Tauride sedimentary platform. Following subduction, the amalgamated SEAOB and Tauride units were accreted to the Arabian margin by mid-Cenozoic time, possibly accompanying transtensional deformation (Robertson 1998; Stampfli 2001). Just how SEAOB was assembled is the subject of ongoing discussion especially for the Late Cretaceous and Early Cenozoic. The main debate is the palaeogeographical position of the Neo-Tethyan Ocean with respect to Eurasian and/or Arabian plates, and the number and evolution of the convergent plate margins that evolved between Arabian and Anatolide–Tauride

platform, which forms the southeastern margin of Eurasian plate. Some authors (Hall 1976; Aktas & Robertson 1984; Dewey *et al.* 1986; Yazgan & Chessex 1991; Yılmaz 1993; Yılmaz *et al.* 1993) argue that the geological events in the SEAOB are rooted in a northerly single ocean that was closed in Late Cretaceous time along a north-dipping subduction zone, followed by thick-skinned re-activation of the suture zone during the Eocene to Miocene. This subduction zone is considered to have generated supra-subduction ophiolites (Goksun, Ispendere, Komurhan, Guleman, etc.) to the south and the Baskil magmatic arc rocks on the active continental margin, the Keban platform, to the north. Conversely, Robertson *et al.* (2005) noted that the Goksun and other ophiolites (Komurhan, Ispendere and Guleman) represent well-developed oceanic crust generated during an inferred mature stage of a suprasubduction zone life cycle, and that the Baskil arc has a large volume of intrusive rocks cutting the Malatya–Keban platform. Based on these constraints, they argue that it is unlikely a single subduction would be sufficient to generate two well-developed tectonomagmatic events in the region. Based on these arguments, others (Robertson 1998, 2000, 2002; Beyarslan & Bingol 2000; Parlak *et al.* 2004; Robertson *et al.* 2005) propose a multiphase convergence along two subduction zones within the Neo-Tethys Ocean. In this model, the ophiolite and related units in SE Turkey formed during these subduction and collisional events related to the consumption of the Neo-Tethyan Ocean along two subduction zones, one a supra-subduction or an intra-oceanic subduction zone and the second a north dipping subduction zone beneath the continental margin of the Malatya–Keban platform to the north. Intra-oceanic subduction on the south accreted the Goksun and other ophiolites (Komurhan, Ispendere and Guleman) to the overriding oceanic plate. Subduction beneath the Malatya–Keban platform generated the Baskil magmatic arc.

## Geological framework of southeastern Anatolian orogenic belt in Baskil-Divrigi transect

The north- to northwesterly-trending Baskil-Divrigi transect, the focus of our investigation, lies between Baskil (Elazig) and Divrigi (Sivas) (Fig. 1). The transect obliquely crosses aligned general NE-trending belts of magmatic rocks in the eastern Tauride terrane. The transect lies oblique to the young sinistral Yakapinar-Goksun fault zone, and is normal to the Bitlis–Zagros suture zone (Figs 1 & 2). Five Late Cretaceous to mid-Cenozoic tectonomagmatic terranes make up the southeastern Anatolian orogenic belt (Fig. 2). These are separated from one another either by major north-dipping thrust faults or by NE-trending strike–slip faults. These terranes are:

(a) Late Cretaceous high-grade metamorphic rocks along the major shortening structures;
(b) Late Cretaceous ophiolitic rocks;
(c) Late Cretaceous active margin units (subduction related magmatic and sedimentary rocks);
(d) Late Cretaceous to Eocene post-collisional to late orogenic magmatic rocks; and
(e) Paleocene–Eocene to Miocene volcanic-sedimentary units.

High-grade metamorphic rocks referred to as the Bitlis-Poturge massif and the Malatya–Keban, Engizek, and Binboga metamorphic rocks (Yılmaz *et al.* 1993; Yılmaz 1993) of Late Palaeozoic–Mesozoic age are the oldest rocks in the basement to the Late Cretaceous and younger rocks. The Bitlis-Poturge massif, exposed mainly at the southern part of the transect (Figs 1 & 2), consists mainly of polydeformed gneiss, amphibolite, and mica schist metamorphosed at greenschist to amphibolite facies conditions (Helvaci & Griffin, 1984; Michard *et al.* 1984, Yazgan & Chessex 1991; Erdem 1994). Amphibole and mica from amphibolites and mica schist within the Bitlis-Poturge massif yielded minimum K–Ar ages ranging from 85–76 Ma and 74–56 Ma, respectively, which represent cooling of the terrane (Yazgan & Chessex 1991). The Bitlis–Pütürge massif is generally regarded either as the northernmost extension of the metamorphic basement of the Arabian margin to the south (Yazgan 1984; Yazgan & Chessex 1991) or as one or several continental fragments rifted from Gondwana in the Triassic during the opening of the Neo-Tethyan oceanic basin (Hall 1976; Sengör & Yılmaz 1981; Robertson & Dixon 1984; Yılmaz 1993; Yılmaz *et al.* 1987; Robertson 1998). Early Cenozoic shallow-water carbonate sequences overlie the massif (Yazgan & Chessex 1991).

Ophiolitic rocks in Baskil-Divrigi transect compose two main groups based on the interpreted palaeogeography of the eastern Mediterranean region, that is the Vardar (Izmir-Ankara-Erzincan) or Neo-Tethyan Oceans. These two basins are separated by continental fragments and unconformably overlain by platform carbonate rocks. Emplacement of ophiolitic rocks and ophiolitic mélanges along north dipping thrust sheets within Divrigi and Keban region probably indicate that these are derived from the northerly ocean, Vardar or Izmir-Ankara-Erzincan Ocean (Fig. 1). This ophiolite complex was emplaced on top of the Keban metamorphic rocks by the latest Cretaceous (*c.* 75 Ma) based on the age of intruding granitoids

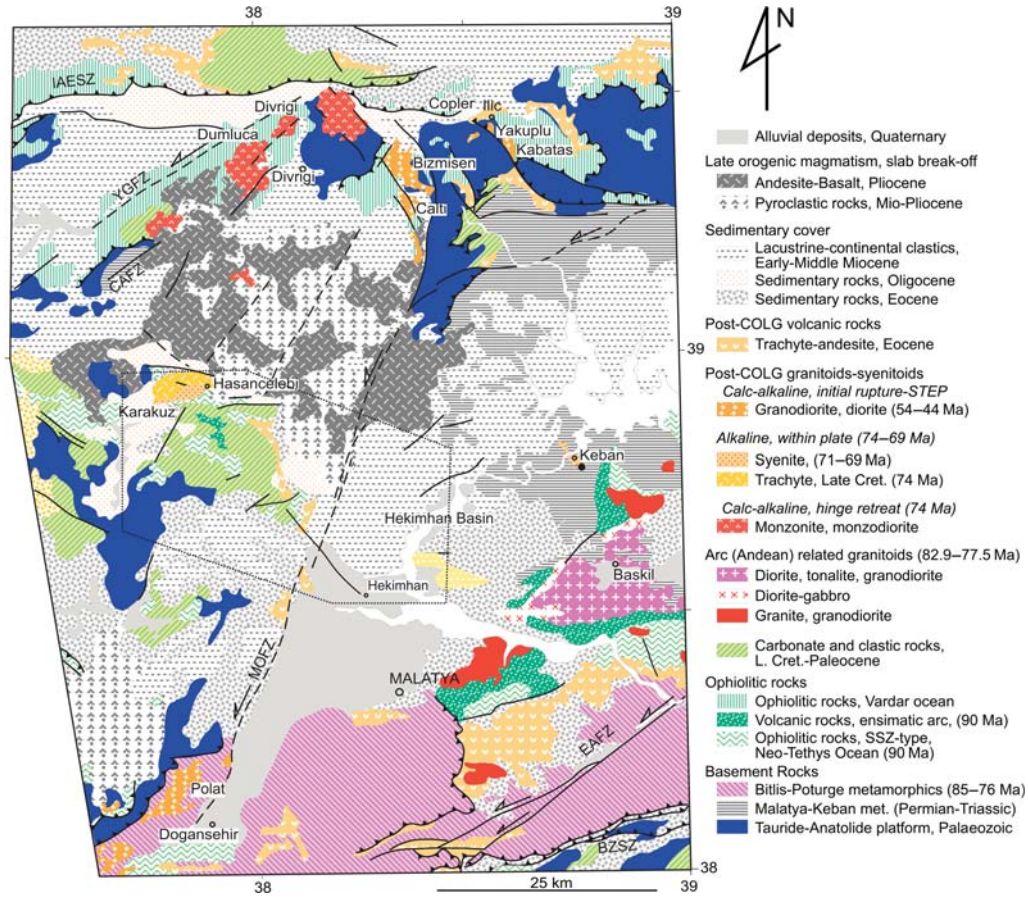


**Fig. 2.** Geological map of Baskil-Divrigi transect (modified from 1/500 000 geological map of Turkey).

(Boztug *et al.* 2005; this study) (Fig. 2). Late Cretaceous to Cenozoic sedimentary and volcaniclastic rocks bury the ophiolite.

Ophiolites mainly in the southern margin of the transect as well as other parts of the SEAOB from Maras to Bitlis are interpreted to have originate as suprasubduction zone (SSZ) ophiolites (Parlak *et al.* 2004, Robertson *et al.* 2005) during the closure of the Neo-Tethyan Ocean. Some of these ophiolites have been metamorphosed to amphibolite facies metamorphism and deformed (Yazgan & Chessex 1991), but nonetheless preserve a coherent ophiolite stratigraphy (Beyarslan & Bingol 2000). Other unmetamorphosed ophiolites, the Guleman and Ispendere complexes, preserve a complete ophiolite pseudostratigraphy, from ultramafic rocks underlain tectonically by a metamorphic sole to volcanic rocks. The high-grade metamorphic sole rocks, preserving an inverted metamorphic gradient, are observed in the Dogansehir (Malatya) region in tectonic contact with overlying ophiolitic units. According to Parlak *et al*. (2004), the metamorphic sole is likely to be equivalent of the Berit metaophiolite (Perincek & Kozlu 1984; Genc *et al.* 1993), found farther to the SW in the Goksun–Afsin (Kahramanmaras) region. K–Ar isotopic age determination on the amphibole from the amphibolite facies yielded a cooling age of 90 $\pm$ 7 Ma (Parlak *et al.* 2004).

The Malatya–Keban metamorphic terrane, outcropping only at the central and northern part of the transect (Fig. 2), is underlain by low-metamorphic grade rocks consisting of slate, phyllite, quartzite, metapelite, calcareous schist, and marble. They represent the Late Palaeozoic to Mesozoic (Ozgul *et al.* 1981) carbonate rock dominated platform sedimentary rock succession that formed part of the Tauride Platform located along the northern margin of the Neo-Tethys. These rocks were metamorphosed to greenschist facies beneath ophiolitic nappes and ophiolitic melange derived from the Vardar (Izmir-Ankara-Erzincan)

Ocean and then exhumed by latest Cretaceous time (Robertson *et al.* 2005). The fault separating these two terranes is interpreted to be a remnant of the subduction zone. Late Cretaceous–Cenozoic post-collisional granitoids intrude the metamorphic terrane.

The active margin, the Baskil arc (Aktas & Robertson 1984; Yazgan & Chessex 1991) or Elazig magmatic suite (Beyarslan & Bingol 2000), consists predominantly of calc-alkaline volcanic and plutonic rocks of Coniacian to Early Campanian age (Yazgan & Chessex 1991; Parlak *et al.* 2001), that locally intrude the suprasubduction zone ophiolites, the structurally overlying Malatya–Keban metamorphic rocks, Bitlis-Poturge metamorphics and the fault contact between the ophiolitic and metamorphic rocks (Perincek & Kozlu 1984; Robertson *et al.* 2005). These granitoids thus postdate ophiolite accretion and must result from north-dipping subduction beneath the Malatya–Keban metamorphic rocks and the Tauride platform (Yazgan & Chessex 1991; Beyarslan & Bingol 2000; Parlak *et al.* 2004; Robertson *et al.* 2005). Published K–Ar geochronology of the granitoid rocks range from 85.76 $\pm$ 3.17 to 77.49 $\pm$ 1.91 Ma (Parlak *et al.* 2004; Robertson *et al.* 2005), an age range confirmed by $^{40}Ar/^{39}Ar$ geochronology summarized below. Tonalite, granodiorite, diorite, gabbro and quartz monzonite intruded by younger microdiorite, porphyritic quartz microdiorite, and by aplite and lamprophyre dykes compose the remnants of the Baskil arc.

The late- to post-orogenic and within-plate magmatic rocks in the transect consist, in general, of late Cretaceous calc-alkaline to alkaline volcanic and intrusive rocks, along with derivative volcaniclastic rocks, and Early to Middle Eocene late-orogenic calc-alkaline magmatic rocks. These rocks postdate ophiolite obduction and unconformably overlie or intrude the metamorphic massifs mainly central and northern parts of the transect. Syenite, syenodiorite, monzonite, phonolite, granodiorite, diorite, monzodiorite and gabbro compose the varied intrusive complexes (Kuscu *et al.* 2007). Spatially, the calc-alkaline suites are generally older and outcrop along the northern margin of the transect. The alkaline suites, however, are younger and generally accompanied extension-related basin formation and deposition of volcaniclastic sequences where they occur as sills or dykes and plugs. These are most common in the Hasancelebi-Hekimhan basin and within Keban region. In general, the nature of magmatism shifts from calc-alkaline to alkaline from north to south (Kuscu *et al.* 2007), a progression of magmatic composition which might be explained as a consequence of gradual change in the geometry of subduction and slab roll-back followed by a possible slab rupture during the advanced stages of subduction and ophiolite obduction (see below).

Volcanic-sedimentary sequences in the Baskil-Divrigi transect are included in two distinct units, the Late Cretaceous to Eocene rocks of the Hekimhan Basin and the Middle Eocene Maden group. The Hekimhan basin (Fig. 2) referred to as a piggy-back basin (Gurer & Aldanmaz 2002) formed above the obducted ophiolitic nappe that roots in the Vardar (Izmir-Ankara-Erzincan) Ocean. Extensional basin formation is considered to have been driven by slab roll-back following the collision and obduction of ophiolites from Vardar (Izmir-Ankara-Erzincan) Ocean. Late Cretaceous to Paleocene continental to shallow marine sedimentary rocks overlain by Paleocene to Eocene marine sequences fill the gradually subsiding basin. Late Cretaceous alkaline sill and dyke complexes and pyroclastic rocks are present in the lower parts of the basin. In contrast, the younger Maden group consists of deep-marine sedimentary rocks, volcaniclastic rocks, and olistostromes, possibly representing a short-lived extensional basin floored by the metamorphic basement (Yılmaz *et al.* 1993; Yigitbas & Yılmaz 1996; Beyarslan & Bingol 2000). Basin formation is generally considered to have formed in either a back-arc basin (Yılmaz *et al.* 1993) or pull-apart basin (Aktas & Robertson 1984). Regardless of the tectonic scenario, it appears as if the Neo-Tethyan Ocean basin remained open with subduction continuing in southeastern Turkey into Cenozoic times (Kaymakci *et al.* 2006).

## Temporal and spatial evolution of magmatism in the Southeastern Anatolian Orogenic Belt

The tectonic setting, age, type and composition of the magmatic rocks vary temporally (Table 1) and spatial along the Baskil-Divrigi transect. Calc-alkaline, active margin-type rocks (Baskil arc) predominate mainly at the south. Igneous rock compositions progressively resemble post-collisional, late-orogenic to within-plate magma (see below) towards the northern part of the transect. The magmatic activity in the Baskil-Divrigi transect initiated at the southern border of the SEAOB with the intrusion of large monzodiorite, granodiorite-granite body into Malatya–Keban metamorphic complex and the suprasubduction-type ophiolitic rocks. $^{40}Ar/^{39}Ar$ geochronology on hornblende and biotite from these intrusive rocks yielded an age from 82.9 $\pm$ 0.4 to 79.4 $\pm$ 0.6 Ma (Table 1), similar to published K–Ar ages between about 85 to 77 Ma (Parlak *et al.* 2004; Robertson *et al.* 2005). A 3 Ma period of apparent

**Table 1.** *Ar/Ar, K–Ar and U–Pb dating on selected magmatic rocks in the Baskil-Divrigi transect (shown are weighted mean or plateau and concordia ages; uncertainities $\pm 2\sigma$)*

| Magmatic rock/pluton | Rock type | Ar/Ar ages | | | | U-Pb | K-Ar |
|---|---|---|---|---|---|---|---|
| | | Hornblende | Biotite | K-feldspar | Sericite | Zircon | Biot-hornb. |
| Horozkoy | Granodio. Q-monzodiorite | 47.17 ± 0.69 | 54.3 ± 1.7 | | | | |
| | Gradio-Q-monzonite | | 50.44 ± 0.28 | | | | |
| Karamadazi | Granodio-monzodiorite | 48.74 ± 0.67 | | | | | |
| | Diorite-monzodiorite enclave | 46.58 ± 0.82 | | | | | |
| Baskil | Monzodiorite | 81.1 ± 1.0 | | | | | |
| | Granite porphyry | 80.15 ± 0.51 | | 72.26 ± 0.62 | | | |
| | Granite Q-porphyry | 79.43 ± 0.58 | | | | | |
| | Granite Q-porphyry with enclave | | | | | | |
| | Q-monzodiorite | | 82.90 ± 0.43 | | | | |
| Keban | Syenite felds. porphyry with metamorphic xenoliths | | | | | 69.9 ± 0.5 | |
| | Syenite felds. porphyry with F veining | | 74.08 ± 0. | 71.85 ± 0.5 | | | |
| Hasancelebi | Trachyte-trachy andesite | | 76.84 ± 0.6 | | | | |
| | Syenite felds. porphyry | | | 71.85 ± 0.5 | | | |
| | Syenite porphyry | | | 70.48 ± 0.42 | | 71.3 ± 0.5 | |
| | Diabase dyke | 74.40 ± 0.51 | 74.32 ± 0.4 | | | | |
| | Syenite porph. intruding ophiolites | | | | | 69.0 ± 0.4 | |
| Divrigi | Q-syenite | | | | | | 76.6 ± 0.6† |
| | Granite | | | | | | 77.2 ± 1.8† |
| | Monzonite-monzodiorite | | 73.48 ± 0.40 | | | | |
| | Monz.-monzodior | | 73.50 ± 0.40 | | | | |
| | Granite with biotite phenocrysts | | 73.40 ± 0.39 | | | | |
| Copler | Microdiorite-diorite porphyry | 44.43 ± 0.61 | | | | | |
| Kabatas | Sericitized granodiorite | | | | 48.63 ± 0.62 | | |
| | weakly seritized microdio. Porph. | | 48.51 ± 0.34 | | | | |
| Doğanşehir | | | | | | | 48‡ |
| Çaltı | Q-diorite | | | | | | 44.7 ± 0.9* |
| Bizmişen | Granodiorite, tonalite | | | | | | 48.8 ± 0.9* |
| | | | | | | | 43.7 ± 0.9* |
| | | | | | | | 46.3 ± 0.4* |

*Data from Onal *et al.* 2005;
†Boztug *et al.* 2007;
‡Parlak *et al.* 2006.

**Table 2.** *Representative geochemical analyses of the magmatic rocks in the Baskil transect*

| Sample | 534664 | 534667 | 534673 | 534674 | 534677 | 534688 | 534693 | 534698 | 535304 | 535312 | 535316 | 535317 |
|---|---|---|---|---|---|---|---|---|---|---|---|---|
| | Horozkoy | | Karamadazi | | | Baskil | | | | Keban | | |
| (wt%) | | | | | | | | | | | | |
| $SiO_2$ | 70.58 | 66.71 | 62.29 | 63.49 | 75.83 | 67.01 | 73.00 | 50.13 | 72.06 | 63.14 | 65.44 | 65.44 |
| $TiO_2$ | 0.27 | 0.35 | 0.71 | 0.62 | 0.13 | 0.27 | 0.28 | 0.92 | 0.31 | 0.28 | 0.34 | 0.37 |
| $Al_2O_3$ | 15.24 | 16.93 | 15.14 | 17.52 | 12.79 | 15.8 | 13.9 | 19.12 | 14.15 | 18.47 | 17.25 | 17.00 |
| $Fe_2O_3^T$ | 3.59 | 5.25 | 8.62 | 4.81 | 0.90 | 6.55 | 4.57 | 19.2 | 4.49 | 2.53 | 3.57 | 3.25 |
| MnO | 0.03 | 0.04 | 0.10 | 0.05 | 0.01 | 0.08 | 0.06 | 0.17 | 0.06 | 0.04 | 0.03 | 0.03 |
| MgO | 0.68 | 1.03 | 3.66 | 2.4 | 0.02 | 0.95 | 0.75 | 3.44 | 0.76 | 0.15 | 0.48 | 0.28 |
| CaO | 2.25 | 3.33 | 6.24 | 5.62 | 0.48 | 2.47 | 2.17 | 9.94 | 3.03 | 2.20 | 1.89 | 2.25 |
| $Na_2O$ | 4.20 | 4.24 | 4.63 | 6.1 | 3.71 | 3.78 | 3.86 | 2.19 | 3.64 | 5.08 | 4.49 | 4.57 |
| $K_2O$ | 3.08 | 2.58 | 0.75 | 0.2 | 4.55 | 4.80 | 1.65 | 0.25 | 1.84 | 5.32 | 4.35 | 4.32 |
| $P_2O_5$ | 0.10 | 0.14 | 0.21 | 0.23 | 0.01 | 0.07 | 0.04 | 0.06 | 0.04 | 0.06 | 0.09 | 0.12 |
| Total | 99.54 | 100.05 | 100 | 100 | 98.46 | 99.96 | 100.05 | 99.35 | 99.41 | 99.39 | 100 | 99.92 |
| (ppm) | | | | | | | | | | | | |
| Ba | 558 | 592 | 238 | 164 | 28.6 | 438 | 227 | 52.4 | 231 | 2990 | 2480 | 2360 |
| Rb | 91.5 | 62 | 16.2 | 3.6 | 232 | 204 | 39.6 | 4.2 | 41.9 | 180.5 | 152 | 164.5 |
| Sr | 450 | 605 | 825 | 1325 | 20.2 | 187 | 102.5 | 188 | 116 | 1680 | 1375 | 1495 |
| Cs | 1.28 | 0.78 | 0.34 | 0.1 | 4.52 | 4.45 | 0.32 | 0.07 | 0.79 | 3.66 | 2.83 | 4.37 |
| Ga | 16.1 | 17.6 | 15.4 | 16.6 | 15.2 | 15.8 | 12.2 | 19 | 13.2 | 23.8 | 23.2 | 21.9 |
| Tl | 0.5 | 0.5 | 0.5 | 0.5 | 0.5 | 0.5 | 0.5 | 0.5 | 0.5 | 0.7 | <0.5 | 0.5 |
| Ta | 1.2 | 1.1 | 1.1 | 0.9 | 3.4 | 1.5 | 0.1 | 0.1 | 0.1 | 1.9 | 2.7 | 2.6 |
| Nb | 13.4 | 14.7 | 17.8 | 16.6 | 27.1 | 16.6 | 1.7 | 0.8 | 1.5 | 52.9 | 51.7 | 49 |
| Hf | 4 | 5.1 | 4.5 | 4.1 | 4.5 | 5.7 | 3.2 | 1.9 | 2.8 | 11 | 11.3 | 11.2 |
| Zr | 124.5 | 175.5 | 161 | 148.5 | 91.9 | 203 | 96.9 | 54.1 | 74.9 | 337 | 398 | 335 |
| Y | 14.9 | 18 | 23.5 | 19.8 | 10.2 | 24.7 | 17.1 | 24.3 | 17.1 | 16.1 | 22.3 | 20.8 |
| Th | 26.3 | 14.8 | 9.5 | 9.47 | 33.9 | 26.7 | 1.88 | 0.35 | 1.9 | 63.7 | 82.4 | 77.8 |
| U | 5.58 | 2.49 | 2.97 | 3.09 | 6.7 | 4.34 | 0.73 | 0.2 | 0.89 | 17.85 | 17.25 | 14.7 |
| Cr | 20 | 20 | 80 | 40 | 20 | 30 | 20 | 30 | 30 | 20 | 20 | 20 |
| Ni | 9 | 12 | 45 | 17 | 10 | 16 | 11 | 21 | 9 | 10 | 12 | 14 |
| Co | 4.1 | 5.6 | 15.7 | 8.7 | 1 | 7.7 | 5.6 | 28.7 | 5 | 2.4 | 4.9 | 4 |
| V | 35 | 52 | 113 | 88 | 9 | 42 | 62 | 380 | 48 | 52 | 72 | 59 |
| Cu | 5 | 11 | 14 | 7 | 6 | 14 | 8 | 108 | 7 | 6 | 5 | 17 |
| Pb | 5 | 5 | 5 | 5 | 11 | 52 | 19 | 5 | 5 | 27 | 11 | 21 |
| Zn | 29 | 33 | 46 | 57 | 18 | 54 | 35 | 94 | 43 | 49 | 35 | 44 |
| W | 6 | 11 | 3 | 5 | 4 | 5 | 1 | 1 | 3 | 5 | 8 | 10 |
| Mo | 2 | 4 | 2 | 2 | 2 | 2 | 2 | 2 | 2 | 21 | 3 | 3 |
| Ag | 1 | 1 | 1 | 1 | 1 | 1 | 1 | 1 | 1 | 1 | <1 | 1 |
| La | 52.7 | 33.8 | 27.2 | 32.6 | 19.4 | 26.4 | 6 | 2.7 | 6.3 | 61.5 | 83.4 | 82 |
| Ce | 86.5 | 59.6 | 53.1 | 60.1 | 30.3 | 46.2 | 11.8 | 5.8 | 12.4 | 124 | 160 | 151 |
| Pr | 8.02 | 6.19 | 6.13 | 6.55 | 2.44 | 4.81 | 1.44 | 0.91 | 1.48 | 13.8 | 16.95 | 16 |
| Nd | 24.9 | 21.7 | 23 | 24.1 | 6.5 | 16 | 6.1 | 5.1 | 6.1 | 47.1 | 57.9 | 54.5 |
| Sm | 3.14 | 3.46 | 4.39 | 4.05 | 0.73 | 2.9 | 1.62 | 1.87 | 1.46 | 6.92 | 8.67 | 8.38 |
| Eu | 0.75 | 0.98 | 1.18 | 1.13 | 0.16 | 0.56 | 0.42 | 0.79 | 0.49 | 1.3 | 1.72 | 1.66 |
| Gd | 3.37 | 3.52 | 4.5 | 4.26 | 1.1 | 3.24 | 1.84 | 2.56 | 1.9 | 5.8 | 7.31 | 7.19 |
| Tb | 0.39 | 0.48 | 0.64 | 0.56 | 0.14 | 0.53 | 0.37 | 0.53 | 0.37 | 0.56 | 0.77 | 0.8 |
| Dy | 1.7 | 2.47 | 3.78 | 3.04 | 0.76 | 3.07 | 2.18 | 3.73 | 2.27 | 2.34 | 3.71 | 3.31 |
| Ho | 0.4 | 0.56 | 0.78 | 0.65 | 0.23 | 0.78 | 0.51 | 0.82 | 0.53 | 0.46 | 0.66 | 0.62 |
| Er | 1.48 | 1.82 | 2.43 | 2.05 | 0.9 | 2.44 | 1.68 | 2.45 | 1.72 | 1.36 | 2.06 | 2 |
| Tm | 0.22 | 0.28 | 0.33 | 0.28 | 0.17 | 0.4 | 0.26 | 0.34 | 0.24 | 0.14 | 0.29 | 0.24 |
| Yb | 1.74 | 2.12 | 2.27 | 1.88 | 1.54 | 2.89 | 2.08 | 2.36 | 2.08 | 1.04 | 2.1 | 1.8 |
| Lu | 0.3 | 0.35 | 0.37 | 0.3 | 0.31 | 0.47 | 0.4 | 0.4 | 0.34 | 0.17 | 0.3 | 0.29 |

magmatic quiescence (Table 1) appears to have been followed by the resumption of post- to late-orogenic magmatism (Table 1) producing small- to medium-sized isolated intrusions into the Malatya–Keban metamorphic complex and structurally overlying ophiolitic rocks and melange in Divrigi and Hasancelebi regions. These magmatic rocks post-date the ophiolite obduction, and are

| Sample | 535318 | h.celebi | 535321 | 535338 | 535340 | 535452 | 535454 | 535457 | C1 | C6 | K3 |
|---|---|---|---|---|---|---|---|---|---|---|---|
| | Hasancelebi | | | Divrigi | | | | | Copler | | Kabatas |
| (wt%) | | | | | | | | | | | |
| $SiO_2$ | 58.10 | 70.78 | 60.55 | 58.96 | 58.47 | 64.09 | 65.47 | 58.91 | 60.05 | 61.91 | 61.93 |
| $TiO_2$ | 1.32 | 0.91 | 1.08 | 1.08 | 1.19 | 0.63 | 0.52 | 1.05 | 0.62 | 0.65 | 0.59 |
| $Al_2O_3$ | 16.24 | 16.50 | 15.96 | 17.98 | 18.08 | 17.33 | 16.76 | 17.65 | 17.39 | 16.76 | 17.41 |
| $Fe_2O_3^T$ | 5.61 | 3.33 | 2.42 | 7.9 | 8.84 | 3.93 | 5.36 | 7.19 | 4.97 | 6.38 | 7.82 |
| MnO | 0.03 | 0.05 | 0.04 | 0.04 | 0.04 | 0.02 | 0.02 | 0.04 | 0.09 | 0.04 | 0.02 |
| MgO | 2.33 | 1.24 | 1.39 | 2.15 | 2.20 | 1.30 | 1.30 | 2.65 | 1.91 | 1.76 | 2.57 |
| CaO | 4.98 | 4.62 | 4.75 | 4.29 | 4.43 | 2.84 | 2.67 | 4.63 | 8.00 | 4.15 | 2.93 |
| $Na_2O$ | 3.40 | 4.92 | 2.69 | 4.64 | 4.16 | 3.88 | 3.76 | 4.13 | 2.16 | 2.54 | 4.01 |
| $K_2O$ | 6.94 | 5.29 | 8.59 | 4.91 | 4.76 | 5.61 | 5.02 | 4.59 | 3.29 | 2.26 | 1.35 |
| $P_2O_5$ | 0.36 | | 0.26 | 0.32 | 0.35 | 0.21 | 0.19 | 0.36 | 0.26 | | 0.15 |
| Total | 99.95 | 99.73 | 99.52 | 100.05 | 99.86 | 99.33 | 99.81 | 99.62 | 99.94 | 99.52 | 98.66 |
| (ppm) | | | | | | | | | | | |
| Ba | 2940 | 1892.33 | 2500 | 1215 | 1330 | 975 | 914 | 1080 | 865 | 679.33 | 402 |
| Rb | 99.8 | 69 | 102.5 | 153 | 162 | 160.5 | 161.5 | 136 | 74.4 | 49 | 32.5 |
| Sr | 326 | 252 | 257 | 352 | 389 | 311 | 302 | 380 | 715 | 470 | 300 |
| Cs | 2.34 | 0.88 | 0.19 | 1.58 | 1.98 | 1.35 | 1.38 | 1.46 | 3.42 | 1.6 | 0.41 |
| Ga | 21.1 | 23 | 23.1 | 20.3 | 20.6 | 19.6 | 19.4 | 20.3 | 19 | 18 | 17.3 |
| Tl | 0.5 | 0.5 | 0.5 | 0.5 | 0.5 | 0.5 | 0.5 | 0.5 | 0.5 | 0.5 | 0.5 |
| Ta | 2.5 | 2.7 | 2.6 | 2.4 | 2.1 | 2.7 | 2.5 | 2 | 0.6 | 0.63 | 0.7 |
| Nb | 40.8 | 42 | 40.2 | 37 | 31.9 | 29.1 | 26.8 | 30.9 | 8.6 | 9.8 | 10.5 |
| Hf | 8.9 | 8.33 | 9.6 | 5.5 | 4.6 | 4.8 | 6.4 | 7.2 | 3.4 | 3.33 | 2.8 |
| Zr | 341 | 348 | 361 | 224 | 188.5 | 186.5 | 257 | 303 | 127 | 124 | 100.5 |
| Y | 44.3 | 40 | 38.4 | 29.1 | 29.6 | 26 | 23 | 30.5 | 20.8 | 16 | 19.5 |
| Th | 20.4 | 27.33 | 23.1 | 22.8 | 23.5 | 30.5 | 28.4 | 21.2 | 7.49 | 8.22 | 8.98 |
| U | 13.05 | 11.3 | 9.41 | 7.77 | 6.04 | 7.5 | 8.29 | 5.86 | 1.76 | 1.74 | 1.72 |
| Cr | 30 | 20 | 20 | 30 | 30 | 30 | 30 | 50 | 20 | 20 | 20 |
| Ni | 38 | 21 | 18 | 12 | 13 | 15 | 15 | 41 | 10 | 11 | 12 |
| Co | 9.6 | 5 | 4.6 | 9 | 9.8 | 5.7 | 6.9 | 15.8 | 7.9 | 9 | 18.4 |
| V | 113 | 62 | 54 | 98 | 108 | 67 | 57 | 106 | 168 | 161 | 134 |
| Cu | 21 | 13 | 12 | 7 | 10 | 5 | 5 | 26 | 7 | 971 | 2420 |
| Pb | 14 | 8 | 6 | 13 | 30 | 10 | 16 | 11 | 5 | 8 | 7 |
| Zn | 45 | 30 | 29 | 44 | 72 | 32 | 41 | 39 | 42 | 94 | 207 |
| W | 8 | 5 | 1 | 2 | 4 | 3 | 5 | 1 | 3 | 2.67 | 3 |
| Mo | 20 | 9.33 | 6 | 2 | 2 | 2 | 2 | 2 | 2 | 10.67 | 26 |
| Ag | 1 | 1 | 1 | 1 | 1 | 1 | 1 | 1 | 47 | 16.3 | 1 |
| La | 70.2 | 53.7 | 73.5 | 40 | 44.9 | 43.6 | 36.7 | 45.8 | 23.3 | 24 | 21.8 |
| Ce | 145.5 | 107.4 | 139.5 | 77.2 | 93.9 | 87.6 | 69.8 | 95.6 | 44.9 | 43.37 | 36.2 |
| Pr | 15.55 | 11.46 | 13.85 | 8.75 | 10.95 | 9.87 | 7.6 | 11.1 | 5.2 | 5.09 | 4.43 |
| Nd | 52.5 | 39.53 | 45.8 | 33.8 | 39.7 | 34.9 | 26.5 | 39.7 | 21.2 | 19.2 | 16.6 |
| Sm | 9.16 | 7.28 | 7.92 | 6.45 | 6.9 | 6.24 | 4.76 | 7.36 | 4.24 | 3.51 | 3.52 |
| Eu | 2.64 | 2.08 | 2.38 | 1.36 | 1.45 | 1.22 | 0.92 | 1.47 | 1.26 | 0.98 | 1.01 |
| Gd | 9.03 | 7.34 | 8.04 | 6.24 | 6.58 | 6.06 | 4.38 | 7 | 3.99 | 3.36 | 3.74 |
| Tb | 1.3 | 1.07 | 1.08 | 0.88 | 0.92 | 0.83 | 0.69 | 0.94 | 0.57 | 0.46 | 0.58 |
| Dy | 7.2 | 6.27 | 6.13 | 5.23 | 4.98 | 4.48 | 3.54 | 5.08 | 3.46 | 2.7 | 3.6 |
| Ho | 1.5 | 1.34 | 1.29 | 1.03 | 0.98 | 0.88 | 0.73 | 1.06 | 0.68 | 0.52 | 0.72 |
| Er | 4.54 | 4.11 | 3.9 | 3.1 | 2.93 | 2.69 | 2.27 | 3.02 | 2.06 | 1.57 | 2.02 |
| Tm | 0.62 | 0.58 | 0.59 | 0.41 | 0.42 | 0.38 | 0.32 | 0.44 | 0.3 | 0.23 | 0.3 |
| Yb | 4.38 | 3.95 | 3.97 | 2.91 | 2.94 | 2.65 | 2.27 | 3.04 | 2.1 | 1.6 | 2.05 |
| Lu | 0.64 | 0.61 | 0.63 | 0.46 | 0.4 | 0.4 | 0.37 | 0.44 | 0.31 | 0.24 | 0.31 |

thus post-collisional intrusions. Although there is a temporal overlap in products of post-collisional magmatism, $^{40}Ar/^{39}Ar$ geochronology (Table 1) suggests that a Campanian (74.40–73.40 Ma) calc-alkaline magmatic phase was followed by a shift to alkaline magmatism during the Maastrichtian (71–69 Ma, U–Pb zircon ages) (Table 1). Slightly younger calc-alkaline magmatic rocks

with $^{40}Ar/^{39}Ar$ ages of 74.40 ± 0.51 to 73.40 ± 0.39 Ma (Table 1) also intruded the Malatya–Keban metamorphic complex, Tauride–Anatolian Platform, and ophiolitic rocks. Alkaline intrusions into the Malatya–Keban metamorphic complex and northerly derived ophiolitic rocks in the Hasancelebi and Keban regions are dated as 71.0 ± 1.0 to 69.9 ± 0.5 Ma by U–Pb geochronology on zircon. The same rocks have been dated as 74.1 to 71.8 ± 0.5 Ma based on $^{40}Ar/^{39}Ar$ dating on biotite (Table 1).

Still younger felsic to intermediate calc-alkaline shallow intrusions present mainly along left-lateral strike–slip faults (CAFZ and YGFZ and MOFZ) associated with sub-basins bounded by these faults or their splays at Copler, Kabatas, Bizmisen-Calti, Karamadazi, Horoz regions yielded $^{40}Ar/^{39}Ar$ ages at 54.3 ± 1.7 to 44.43 ± 0.61 Ma (Table 1). These rocks crop out as isolated plutons that post-date collision of the Pontides with Tauride–Anatolian Platform and obduction of northerly ophiolites from the Vardar Ocean. The available geochronology from this study and other studies by K–Ar geochronology (Onal *et al*. 2005; Parlak *et al*. 2006; Table 1) also show Eocene magmatism is essentially continuous from Late Paleocene to Eocene (early Ypresian to late Lutetian), and contemporaneous with basin evolution and sedimentation. The Eocene magmatism in the SEAOB is not confined to Copler, Kabatas, Horoz and Karamadazi granitoids, but is generally widespread, although volumetrically less than the older igneous complexes such as Dedeyazi-Polat (Dogansehir) and Bizmisen-Calti granitoids. The K–Ar geochronology on magmatic hornblende/biotite yielded an age of *c*. 48 Ma (Parlak *et al*. 2006), and 43.7–46.3 Ma (Onal *et al.* 2005), respectively.

Onal *et al.* (2005) dated the Eocene post-collisional granitoids in Bizmisen and Calti (Divrigi, Sivas) plutons as 42–56 Ma to 40–49 Ma. Similar Eocene magmatic rocks are also reported in Iran along the eastern continuation of the Bitlis–Zagros subduction zone where Urumieh-Dokhtar magmatic belt formed as a consequence of slab break off during the Middle Eocene (Bird 1978; Ghasemi & Talbot 2005). Yigitbas & Yılmaz (1996) and Robertson *et al* (2005) also described Eocene magmatism in the Maden Complex and Helete volcanics, and postulated an arc and back-arc setting for their formation, respectively. Eocene magmatism discussed herein is located north of the arc-related rocks of Late Cretaceous age, and is unrelated to the Maden Complex and Helete volcanics.

In summary, the $^{40}Ar/^{39}Ar$ geochronology (Table 1) along with geochemical characteristics of the granitoids (see below) indicate a geographic shift in the magmatic loci was coupled with a transition from arc-type calc-alkaline to post-collisional calc-alkaline to alkaline then to within-plate alkaline magmatism with time from 82.9 ± 0.4 to 79.9 ± 0.6 Ma, 74.40 ± 0.51 to 73.40 ± 0.39 Ma to 71.0 ± 1.0 to 69.9 ± 0.5 Ma from south to north, respectively. These igneous complexes are subsequently overprinted by post-collisional calc-alkaline magmatism at 54.4–44.3 Ma (Table 1) mainly along a NE-trending belt located in the central part of the transect. Available geochronologic data suggest each individual magmatic period has a relatively short lifetime of *c*. 2–5 Ma.

## Geochemical characteristics of the magmatic rocks in Baskil-Divrigi transect

Magmatic rocks in Baskil-Divrigi transect are sub-alkaline and alkaline but have significant scatter due to wide range of compositional diversity (Table 2; Fig. 3). Baskil magmatic rocks have both a felsic and a mafic end-member. The mafic and felsic end-members appear to follow a tholeitic and calc-alkaline trend, respectively (Fig. 3b). In general, the Horoz, Karamadazi, Copler and Kabatas (Yakuplu) granitoids have subalkaline characteristics with more calcic affinities (Fig. 3c) whereas Keban and Hasancelebi volcanic-plutonic rocks have alkaline characteristics with a calcic to calc-alkaline affinity. Variable A/CNK [molar $Al_2O_3/(CaO + Na_2O + K_2O)$] and A/NK [molar $Al_2O_3/(Na_2O + K_2O)$] characterize the complexes. The magmatic rocks in Baskil and Copler-Kabatas are peraluminous whereas in Hasancelebi, Divrigi, Karamadazi and Horoz regions, these rocks are metaluminous (Fig. 3d). In general, the granitoids in Baskil, Copler and Kabatas are medium-K suites whereas the Hasancelebi and Divrigi-Murmano plutons are high-K to shoshonitic (Fig. 3e). The Divrigi-Murmano pluton has compositions that suggestion both alkaline and calc-alkaline; field relations and petrographical observations indicate the extreme compositional heterogeneity in these is due to alkali metasomatism (scapolite-albite alteration overprinted by K-feldspar and phlogopite) of a $20 \times 5\ km^2$ region that is associated with a large ($>10^8$ tonnes) IOCG deposit (Kuscu *et al.* 2002, 2007).

The magmatic rocks range from basalt-gabbro to syenite and trachyte with a common overlap between the compositional fields of Pearce (1996) (Fig. 4a) and Winchester & Floyd's (1977) diagrams (Fig. 4b). In the Baskil region, basalt, diorite, gabbro-diorite and granite to quartz diorite are present. Diabasic dykes at Baskil have distinct compositions characterized by the lowest $Zr/TiO_2$ and Nb/Y ratios recorded in the transect, and plot in

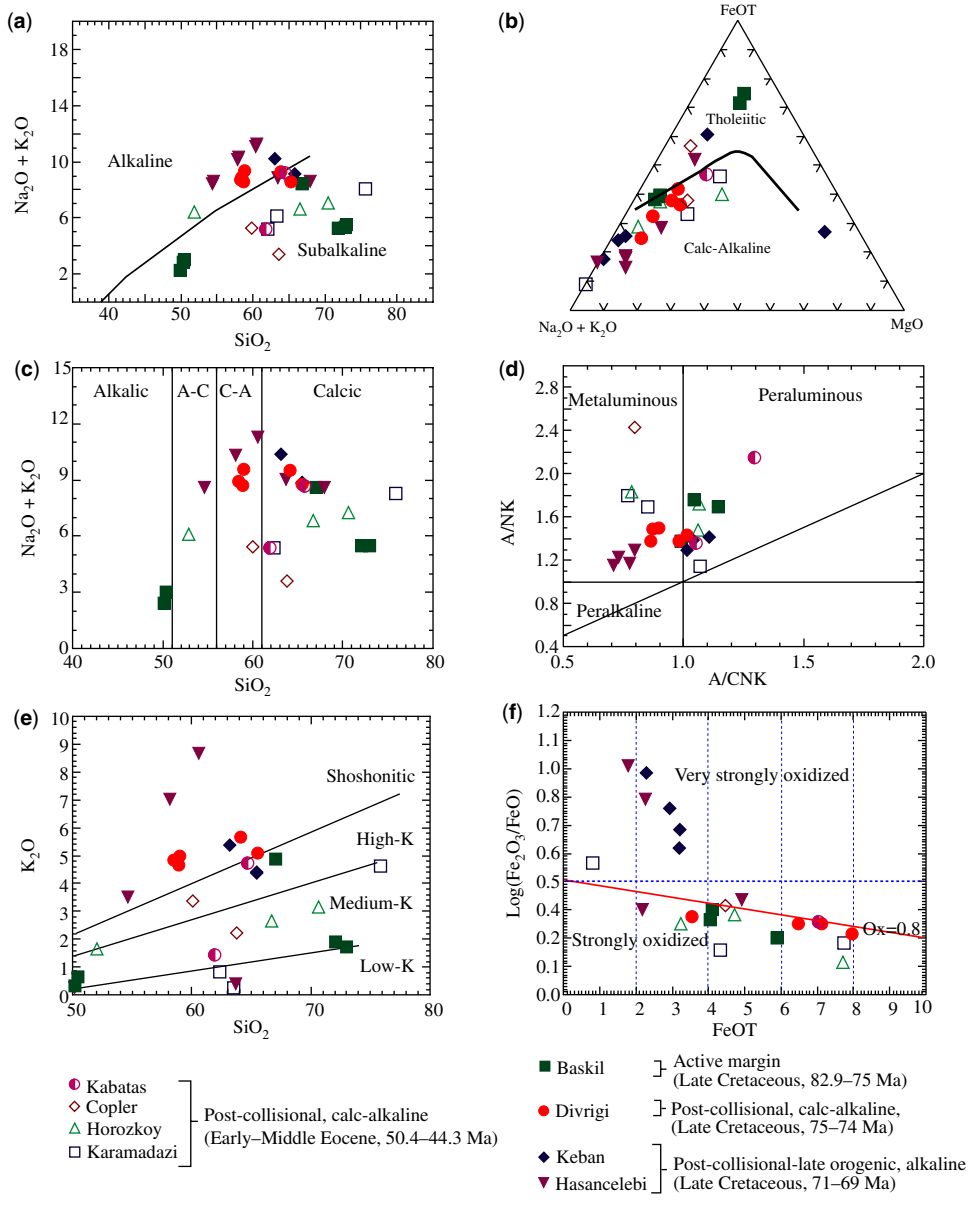


**Fig. 3.** Major element plots of the magmatic rocks. (**a**) Total alkalis v. silica (TAS); (**b**) AFM plots of Irvine & Baragar (1971); (**c**) Peacock (1931) index; (**d**) the Shand's Index of Maniar & Piccoli (1989); (**e**) Gill (1981); and (**f**) oxidation state diagrams of (Blevin & Chappell 1992).

basalt field (Fig. 4a). The Baskil rocks are furthermore characterized by higher $SiO_2$ composition than magmatic rocks in Keban, Hasancelebi and Divrigi regions (Fig. 4b), perhaps reflecting higher degrees of fractionation. Although, the Baskil rocks have compositions similar to other magmatic rocks within the transect, they form a distinct group with low- to medium-K and strongly oxidized compositions (Fig. 3f).

In contrast to the more normal calc-alkaline rocks at Baskil, the magmatic rocks near Keban are mainly syenite and syenodiorite in composition. They have the highest $Zr/TiO_2$ and $Nb/Y$ ratios in the transect (Fig. 4a). At Hasancelebi, trachyte,

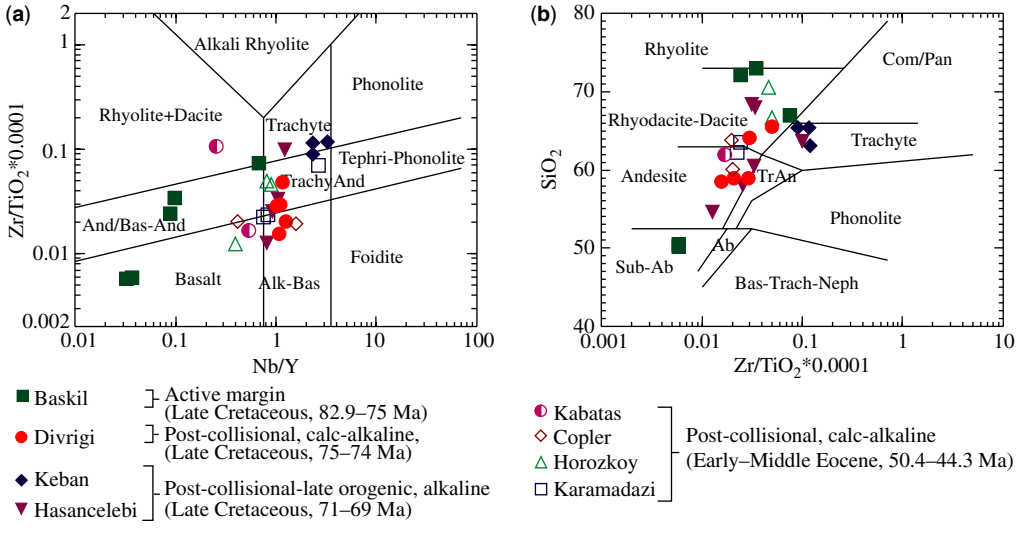


**Fig. 4.** (**a**) Modified $Zr/TiO_2$-Nb/Y plot (Pearce 1996) of Winchester & Floyd (1977), and (**b**) $Zr/TiO_2$-$SiO_2$ plot (Winchester & Floyd 1977).

trachyandesite and syenite to syenodiorite form volcano-plutonic complexes intruding the Late Cretaceous to Paleocene Hekimhan sedimentary basin. The syenites occur as plugs or stocks intruding the ophiolitic and trachytic rocks within the basin. Magmatic rocks in Copler-Kabatas plutons and Divrigi-Murmano share similar compositional ranges, from gabbro, diorite, monzodiorite to granodiorite in composition. Similar compositional ranges are present in the Karamadazi and Horoz regions (Fig. 4a). However, those in the Horoz region tend to contain higher $Zr/TiO_2$ ratios and $SiO_2$ compared to Karamadazi, Copler and Kabatas regions.

### *Trace element-REE geochemistry*

Magmatic rocks in the Baskil transect contain moderate to low HFSE (high field strength elements such

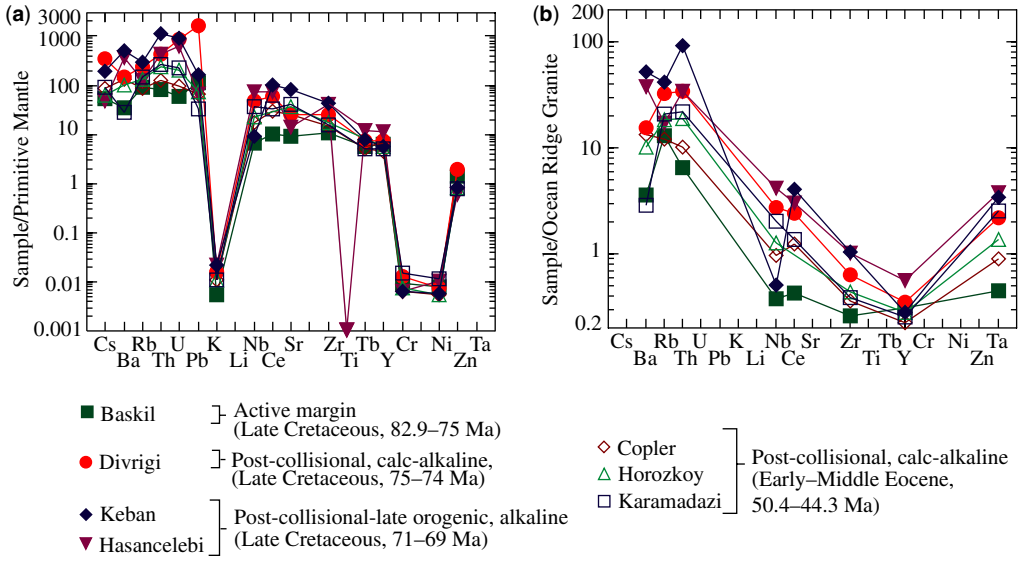


**Fig. 5.** (**a**) Rock/primitive mantle-normalized, and (**b**) rock/ocean ridge granite-normalized (Pearce *et al.* 1984) spidergrams.

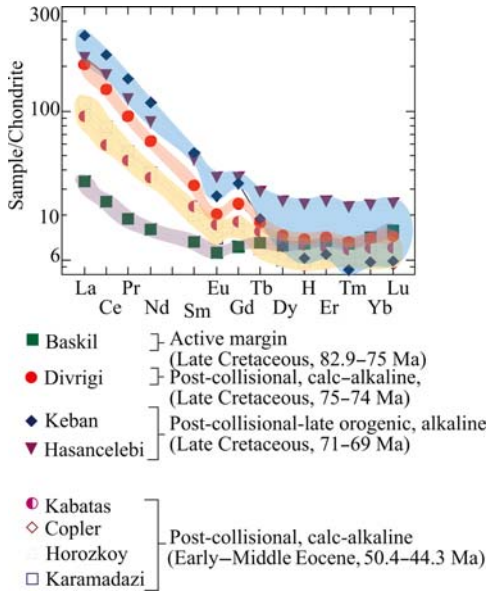


**Fig. 6.** Rock/chondrite normalized average REE plot of the magmatic rocks from the central-eastern sector.

as Nb, Ta, Ga, Zr, Hf, Y) indicating an arc to post-collisional/late-orogenic setting for their generation (Figs 5a, b). Primitive mantle-normalized extended trace element spiderplots (Fig. 5a) are characterized by large ion lithophile element (LILE) enrichment with respect to HFSE, and strong negative K and Cr-Ni anomalies. The LILE enrichment in the magmatic suites other than Baskil arc is more pronounced. Ocean ridge granite-normalized plots, used to compare arc-related rocks with rocks in the eastern-central transect (Fig. 5b), illustrates a moderate negative Y, Zr and Nb (HFSE) anomalies, and positive Rb and Th anomalies in all rocks. In general, the Copler and Kabatas plutons, Karamadazi and Horoz granitoids are characterized by depleted Nb and Zr contents (Fig. 5b). In contrast, the Divrigi-Murmano pluton and Hasancelebi volcano-plutonic rocks are characterized by moderate Nb and Y contents. Syenitoids in the Keban region have the highest Nb and Zr contents measured in the transect (Fig. 5a, b).

The negative Nb anomalies in the Baskil transect rocks are common features of rocks associated with arc lavas and incipient back-arc basin basalts due to the influx of low field strength element (LFSE) into the mantle source regions from the subducted slab (Wilson 1989). As is commonly accepted, arc magmatism derives mainly from the melting of subducted oceanic crust, overlying mantle wedge and lower continental crust. Such magma will essentially reflect the inherited geochemical signatures of these source regions, as these source materials can also be melted in a post-collisional environment. Other trace element characteristics of subduction-related magmas include enrichment in Ba, Th and Pb, and depletion in Nb in addition to Ti and Ta (Fitton *et al.* 1988; Saunders *et al.* 1980, 1988). Of them, Nb and Ta are also highly sensitive to crustal contamination. Mantle-derived magmas, which might be contaminated by continental crustal rocks during their ascent to the surface, have marked Nb and Ta negative anomalies (Wilson 1989). Therefore, the negative Nb anomaly on these plots need not reflect an arc environment. Nonetheless, the trace element geochemistry does indicate a subducted slab component is present in these rocks. The rocks are generally enriched in light rare earth elements (LREE) relative to chondrites (Nakamura 1974), but to differing extents (Fig. 6). All samples are characterized by significant flattening of heavy rare earth element (REE) patterns relative to the LREE, and a marked depletion in Eu. La/Sm in Baskil magmatic rocks is less compared to other igneous suite, suggesting a distinct environment for the generation of these rocks. Likewise, the Eocene Horoz, Copler, Kabatas and Karamadazi display almost the same REE patterns implying a common mechanism or source for their generation. Rocks in Hasancelebi, Divrigi and Keban have similar LREE patterns but distinct HREE (heavy rare earth element) patterns with a flatter HREE pattern for Hasancelebi. In addition, REE also show three distinctive groups, principally based on LREE compositions (Fig. 6); these groups are almost the same as those defined by trace elements (see above), and differ from each other by their relative LREE enrichment with respect to HREE and to chondrite (Fig. 6). The Late Cretaceous rocks from the Baskil region define a group with the lowest rock/chondrite ration, and are characterized by a slight enrichment in terms of LREE. The Eocene magmatic rocks in Copler, Kabatas, Karamadazi and Horoz regions constitute the second group, and have a moderate LREE enrichment. The third group has higher LREE enrichment, and includes the latest Late Cretaceous magmatic rocks from Keban, Hasancelebi and Divrigi regions. Combining with the distinct ages for the magmatic rocks, these chemical groups provide further evidence that different magma generation events were active at different times, and these also likely reflect different tectonic environments (see below).

Ta/Yb, Th/Yb, Th/Y, Nb/Y, and Nb/Zr ratios and their comparison on suitable binary plots may be useful in assessing the role of source heterogeneities, metasomatism and crustal contamination (Pearce 1983) (Fig. 7a, b) in the generation of magmas. All magmatic rocks within the transect have trends in Th/Yb v. Ta/Yb that parallel the

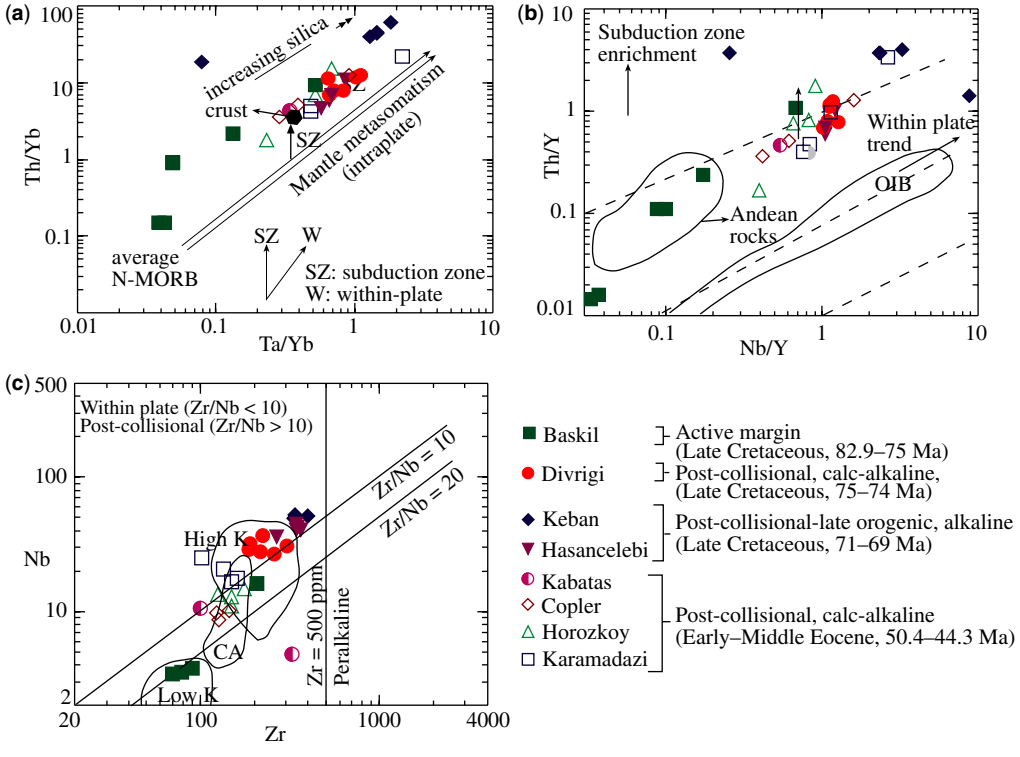


**Fig. 7.** (**a**) Th/Yb v. Nb/Y diagram showing the rocks from Andean subduction zone, and from the eastern-central transect; (**b**) Th/Yb v. Ta/Yb diagram (Pearce 1983) showing the effect of mantle metasomatism (crust average for central Anatolia were taken from Ilbeyli 2005); and (**c**) Nb-Zr plot of Leat *et al.* (1986) showing within-plate component.

mantle metasomatism array, but are displaced towards higher Th/Yb ratios. In addition, both ratios increase from the calc-alkaline through alkaline intrusive rocks. The alkaline syenitic rocks in Keban region contain higher Ta/Yb and Th/Yb ratios compared to Hasancelebi region, and to the calc-alkaline plutonic rocks in Copler, Kabatas, Karamadazi, Horoz, and Divrigi regions. The magmatic rocks in Baskil plot at low Th/Yb and Ta/Yb ratios with lowest Ta/Yb ratios that may be indicative of subduction-related setting (Pearce 1983). The remaining magmatic rocks, display moderate Th/Yb and Ta/Yb ratios suggesting a derivation from a metasomatized mantle inherited from an earlier subduction, likely reflecting a post-collisional or late-orogenic setting.

The Th/Y v. Nb/Y diagram (Fig. 7b) distinguishes within-plate source from subduction-related source regions. Mantle that has been enriched by subduction components and/or crustal components shift to higher Th/Y ratios with respect to Nb/Y, whereas mantle previously enriched by a small volume of partial melt is displaced along the melt enrichment and within-plate trend in the direction of high Th/Y and Nb/Y ratios (Pearce 1983) (Fig. 7b). Most felsic magmatic rocks at the Baskil region plot in mantle metasomatism array with increasing Th/Y and Nb/Y ratios suggesting melt enrichment and within plate signature most probably derived from a lithospheric mantle source carrying an older subduction component. Of particular importance, the Horoz, Karamadazi and Copler intrusions have a weak subduction zone enrichment array (Fig. 7a, b), that we infer to be inherited from an older subduction event, or melting of a source that could be of an older subducted slab, or mantle wedge contaminated by a subduction component. A similar behaviour is observed in an Nb v. Zr diagram (Fig. 7c) which has been proposed to characterize the geochemical and tectonic setting characterization of felsic rocks (Leat *et al.* 1986). Depletion in Zr and Nb concentrations coupled with increasing Zr/Nb ratios is typical of arc-related rocks. Likewise, a gradual increase in Nb and corresponding decrease in Zr/Nb ratio cause shift toward post-collisional setting to within plate settings (Fig. 7c). The Baskil arc-type rocks plot in high Zr/Nb with ratios. Copler, Kabatas and Horoz granitoids plot in moderate Nb and Zr concentrations, which indicate

this magmatism is related to a source modified by subduction. This magmatic association has been described in provinces such as Snowdonia, Avoca and Parys Mountain, within the Southern British Caledonides (Leat *et al.* 1986). The magmatic rocks in Divrigi, Hasancelebi, Keban and to some extend Karamadazi regions have Zr/Nb ratios $<10$ with highest Nb and Zr concentrations which collectively suggest an anorogenic setting. However, as discussed previously, the alkalinity and consequent geochemical signature in Divrigi-Murmano pluton is due to a pervasive hydrothermal alteration (alkali metasomatism) that affected the entire pluton. Alkaline syenitoids in Keban always plot in the highest Nb and Zr corner of the diagrams suggesting these were derived from within plate setting modified by a subduction zone component.

Magmatic suites in Baskil-Divrigi transect are clustered in three overlapping groups based on compositions and ratios of Nb, Zr, Th, Y, Ta and Yb in Figure 7a–c. These may represent grouping of granitoids formed during different tectonic settings. The high Th/Yb-Ta/Yb and Th/Y-Nb/Y and high Zr/Nb ratios (group 3) in Keban region are typical for within plate settings whereas, low Th/Yb-Ta/Yb, Th/Y-Nb/Y and high Zr/Nb (group 1) ratios are typical for low-K arc-related granitoids exposed mainly in the Baskil region. The other magmatic rocks from the Karamadazi, Horoz, Divrigi, Hasancelebi, Copler and Kabatas regions are clustered at moderate Th/Yb-Ta/Yb, Th/Y-Nb/Y and Zr/Nb ratios (group 2) in between the within-plate and the arc-related settings. Some of the samples from Baskil have Th/Y and Nb/Y that is similar to rock defining an Andean rock field (Pearce 1983).

### *Petrogenesis and tectonomagmatic classification*

Possible tectonic environments for the Baskil magmatic rocks can be generally inferred based on trace and REE characteristics using classical tectonomagmatic discrimination diagrams (Fig. 8e, f), coupled with other geological evidence. Although not completely conclusive in discriminating the complex tectono-magmatic settings, trace element and REE characteristics coupled with multi-element variation diagrams suggest three main petrotectonic settings for the generation of the magmatic rocks in Baskil-Divrigi transect. These are: (1) subduction and arc setting and (2) post-collisional and extensional setting (exhumation, probably due to roll-back) followed by (3) late-orogenic extension, probably due to crustal scale strike–slip faulting or subduction transfer edge propagator (STEP)-faulting (as defined in Wortel & Spakman 2000). The magmatic rocks from the Baskil, Copler, Kabatas, Karamadazi and Horoz all plot mainly within the VAG and pre-plate collision fields with a marked input from the mantle by their narrow Y and Y + Nb, and low Rb and Ta compositions (Fig. 8a–f; Pearce *et al.* 1984; Pearce 1996; Batchelor & Bowden 1985). Magmatic rocks in the Baskil region are of arc-type (Hall 1976; Aktas & Robertson 1984; Dewey *et al.* 1986; Yazgan & Chessex 1991; Yılmaz 1993; Yılmaz *et al.* 1993; this study) that post-date the collision between Malatya–Keban metamorphic rocks and ensimatic arc/ophiolite (Beyarslan & Bingol 2000; Parlak *et al.* 2004; Parlak 2005; Robertson *et al.* 2005). Northward subduction of SSZ-type oceanic crust during the evolution of the southern branch of the Neo-Tethyan Ocean generated the arc (Hall 1976; Aktas & Robertson 1984; Dewey *et al.* 1986; Yazgan & Chessex 1991; Yılmaz 1993; Yılmaz *et al.* 1993; Beyarslan & Bingol 2000, Parlak *et al.* 2004; Robertson *et al.* 2005). Subduction of the northern margin of Arabian platform beneath the southern passive margin of Tauride–Anatolide platform during latest Cretaceous time marked the cessation of arc magmatism.

Late Cretaceous magmatic rocks in Divrigi, Hasancelebi, and Keban have compositions suggestive of a post-collisional setting with a common overlap to within plate setting. Commonly, late-orogenic extensional regimes generated during collision and collision-induced roll-back of the subducting slab will produce post-collisional granitoids of diverse type and origin; these are the post-COLG and late-orogenic granitoids on the Pearce (1996) and Batchelor & Bowden (1985) diagrams, respectively (Fig. 8b–d). In eastern Turkey, these Late Cretaceous granitoids intrude the Malatya–Keban metamorphic rocks and structurally overlying ophiolitic nappes, and are post-collisional. Hinge retreat or roll-back, which likely followed collision, appears to be active when continental lithosphere of the Arabian plate subducted beneath the southern margin of the Anatolide–Tauride platform (continental collision).

The syenitic rocks in Keban and Hasancelebi region show geochemical features characteristic to within-plate setting (Fig. 8a–f). The ternary Nb-Y-Ga diagram (Fig. 8e) of Eby (1992) suggests these magmas were derived from partial melting of mantle material. As melting conditions in mantle require generally excess water and rapid decompression, an influx of fluids from subducted slab and rapid removal of pressure by slab roll-back mechanisms appear to be required. Implicit in this model is the hypothesis that generation of alkaline rocks accompanied extensional tectonism related to advanced stages of slab roll-back.

An arc origin can be inferred for the Eocene magmatic rocks in Copler, Kabatas, Karamadazi

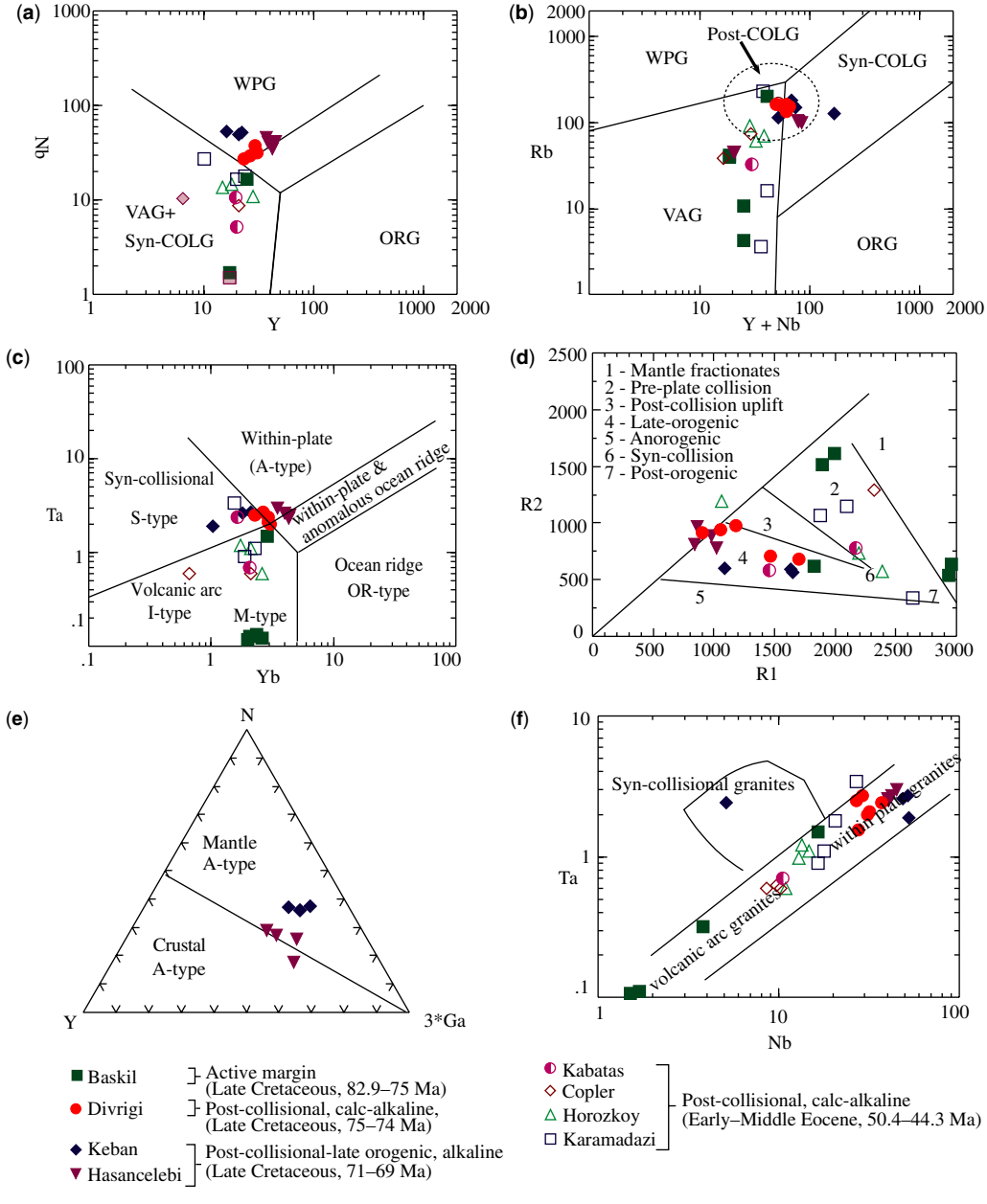


**Fig. 8.** (**a**) Nb-Y; (**b**) Rb − Nb + Y; (**c**) Ta-Yb diagrams of Pearce *et al.* (1984), Pearce (1996); (**d**) R1-R2 diagram of Batchelor & Bowden (1985); (**e**) Nb-Y-Ga diagram of Eby (1992); and (**f**) Ta v. Nb diagram of Harris *et al.* (1986).

and Horoz regions, based on the tectonomagmatic discrimination diagrams (Fig. 8a–d). Several lines of geological evidence, however, suggest that the arc setting may not be correct for any rocks except for those the Late Cretaceous Baskil granitoids. All of the Eocene magmatic rocks intruded obducted ophiolitic nappes. The relationship suggests that, at a minimum, their emplacement post-dates collision and obduction of the ophiolitic rocks. Furthermore, none of the granitoids have contemporaneous fore-arc sequences or accretionary prism, and no significant high-pressure metamorphism rooted to a subduction event can related in time and space, unlike older arc terranes. Therefore,

concluding an arc origin for the Eocene magmatic rocks based on the geochemical discrimination diagrams appears inconsistent with the available geological evidence. Instead, an arc signature might have been inherited from older subduction events that producing Baskil arc magmatic rocks, or could be attributed to melting of a mantle wedge contaminated by older subduction. If the Eocene rocks are related to subduction, then the available geochronologic constraints requires two subduction events, one in the Late Cretaceous, and the younger one in early to middle Eocene times. Late Cretaceous subduction is well established in the SEAOB. In contrast, the case for subduction in Eocene is subject to conflicting interpretations (Sengör & Yılmaz 1981; Yigitbas & Yılmaz 1996). The Eocene subduction zone proposed by Yigitbas & Yılmaz (1996) would have been located south of Maden complex, which has been interpreted to be a remnant of a back-arc basin filled with volcanic rocks and lacking significant intrusions. Robertson *et al.* (2005) have also proposed that the Eocene Helete volcanics, deposited within an extensional basin above the metamorphic rocks, record subduction but suggest a back-arc setting to be more likely. Richards (2003) suggested that the Urumieh-Dokhtar magmatic belt in Iran, which may be the southeastern continuation of the magmatic rocks in SEAOB, formed by Eocene subduction of southern Neo-Tethyan Ocean beneath the Eurasian plate. In contrast, Ghasemi & Talbot (2005) proposed that the Urumieh-Dokhtar magmatic belt formed as a consequence of slab break-off during middle Eocene. Onal *et al* (2005) also suggested that the Calti and Bizmisen plutons have been formed due to slab break-off. However, an origin via slab break-off for the Eocene magmatism seems to be contradictory in SEAOB. There are several lines of evidence against slab break-off in eastern-southeastern Turkey; Keskin (2003) and Sengör *et al.* (2003) proposed that a slab break-off event related to Afro-Arabian and Eurasian collision took place during middle Miocene (after 11 Ma), significantly after intrusion of the Eocene granitoids. They also put constraints on the magma chemistry and postulated that the magmatism related to slab break-off is more-like plume or OIB-type, which is significantly different from the Eocene magmatism in SEAOB. Furthermore, surface waveform velocity data by Maggie & Priestly (2005) showed that the slab-break-off and resultant delamination processes within the eastern Mediterranean or western Tethys took place at about 12 Ma. Besides, seismic tomography and tectonic reconstructions by Hafkenscheid *et al.* (2006) are all agreement with subduction of Arabian continental lithosphere underneath Eurasia and slab break off around 12 Ma in the Arabian–Tethyan region. Therefore, these are sound evidence ruling out a possible slab break-off event during Eocene in the SEAOB, and a possible slab break-off would not be a driving mechanism for the Early–Middle Eocene magmatism in eastern-southeastern Turkey. Therefore, we suggest that the Early–Middle Eocene magmatism in the SEAOB should have been formed as result of extensional tectonics and crustal scale fractures due most likely to initial slab rupture or STEP faulting during the final re-organization of plate configurations and construction of the NeoTethyan subduction front during Early–Middle Eocene (Stampfli *et al.* 2002; Moix *et al.* 2008). Moix *et al*. (2008) favour a bending of the subduction front from Cyprus to Erzincan mainly at 48 Ma. It is highly likely that the further bending, and continuous north–south push of the Arabian plate caused a rupture at the overriding plate, or tearing along NE–SW trending crustal scale STEP faults, and left-lateral southwards displacement of the subduction front. This displacement is likely to be accommodated by several NE-trending strike–slip faults such as central Anatolian, Sariz-Goksu, and Malatya-Ovacik fault zones since the Early Eocene. This event also resulted in the extensional regime and asthenospheric windows to create magmas with typical arc signatures. The present spatial distribution of the Eocene magmatism in the central, eastern and southeastern Anatolia suggest that these faults acted as loci for the generation and emplacement of Early–Middle Eocene magmatic rocks in the SEAOB.

## Magmatic sources

In general, the geochemical signatures (major, trace and REE elements) and regional geological constraints of all Late Cretaceous–Cenozoic igneous rocks in the Baskil transect mimic the characteristics of magmatic-arc and post-collisional to late-orogenic magmas of subduction to post-subduction-related origin. Overall, the geochemical characteristics of the magmatic rocks suggest a role of metasomatized mantle in their generation and point to major changes in subduction and mantle geometry beneath the subduction-collision zone between Afro-Arabia and Eurasia from 82.9 to 69.9 Ma then to 44 Ma. Wortel & Spakman (2000), Duggen *et al.* (2005), McQuarrie *et al.* (2003), Govers & Worlet (2005), Von Quadt *et al* (2005) and Neubauer *et al.* (2005) argue that Alpine magmatism is a direct consequence of collision between Afro-Arabia and Eurasian plates, and that changes in the subduction geometry resulted in diverse magma types at different time periods. The rapidly changing geochemical

characteristics of the magmas in the Baskil transect are consistent with this model. The proposed large-scale mantle and subduction-collision processes are associated with large-scale extension and contemporary magmatism possessing characteristics of metasomatized mantle signatures. Continental to marine clastic rocks filled the temporally related sedimentary basins.

Metasomatized mantle sources with fundamentally distinct geochemical compositions should have been partially melted in the course of the large-scale reorganization of the upper mantle. Potential sources in the transect could be (1) a shallow mantle wedge consisting of depleted asthenosphere and attenuated continental lithospheric mantle enriched by fluids or melts from subducted oceanic lithosphere beneath the Anatolide–Tauride platform at 82.9–77.5 Ma and (2) metasomatized subcontinental mantle lithosphere beneath the Malatya–Keban platform that had been modified by fluids or melts from the subduction zone or an older subduction event.

Possible magma generation models explaining spatial-temporal evolution of magmatism in SEAOB are: (1) subduction of oceanic lithosphere; (2) roll-back of subducted oceanic lithosphere; and (3) initial rupture or step-faulting of subcontinental mantle lithosphere. The field geological, geochemical and geochronological evidence suggest that these models acted successively from Late Cretaceous to Middle Eocene. Simple subduction can only explain the Late Cretaceous arc-type magmatism in a frontal part of the Baskil arc, on the south. The calc-alkaline to alkaline magmatic rocks mainly in the northern and central part of the transect have geochemical features more akin to late-orogenic settings and metasomatized mantle source, leading us to postulating a roll-back model at $74.40 \pm 0.51$ to $69.9 \pm 0.5$ Ma. The timing of magma emplacement indicated that the roll-back resulted in two successive pulses of magmatism generating calc-alkaline as the first phase and alkaline as the second phase (Fig. 9). The change is proposed to reflect an increase in the angle of bending (hinge retreat) of the subducted slab beneath the Malatya–Keban platform, which would likely enhance regional extension leading to formation of alkaline rocks with more within plate affinity during $71.0 \pm 1.0$ to $69.9 \pm 0.5$ Ma.

Resumption of calc-alkaline magmatism between 54.4 and 44.3 Ma is preserved as isolated shallow-level intrusions lying parallel to left lateral Yakapinar-Goksun, Malatya-Ovacik, and central Anatolian fault zones that might be originated as crustal scale faults during a continental lithospheric subduction. The present spatial distribution of the Eocene magmatism in the central, eastern and southeastern Anatolia suggest that these faults acted as loci for the generation and emplacement of Early–Middle Eocene magmatic rocks in the SEAOB. These also resulted in the extensional regime and generation of asthenospheric windows to create magmas with typical arc signatures inherited from older subduction that created Baskil arc.

## Geodynamic-tectonic evolution

The tectonic environments defined above are related to the northward subduction of African–Arabian plate beneath the Eurasian plate (Anatolide–Tauride platform *sensu stricto*) initiated during the Late Cretaceous (*c*. 90 Ma) and culminating in the Middle Miocene (Robertson *et al.* 2005). Regional geological data suggest that subduction proceeded in two stages; an older episode of northward subduction of oceanic crust of the Neo-Tethyan Ocean beneath eastern Taurides, now represented by the Malatya–Keban metamorphic complex. Ophiolitic rocks and an ensimatic marine arc formed in the supra-subduction zone environment (*c*. 90 Ma). The younger subduction phase beneath these previously accreted oceanic crust and metamorphic complexes produced arc-related magmatism (82.90–79.9 Ma) intruding the ophiolites and metamorphosed platform rocks of Anatolide–Tauride platform. It appears likely that at an advanced stage of subduction either the geometry of the subduction changed or the rate of convergence of Afro-Arabian plates decreased with respect to Eurasian plate. These changes in convergence initiated a roll-back of the subducting slab during the latest Cretaceous leading to regional extensional due of thickened continental crust, and formation of syntectonic basin formation in the overriding continental plate (Fig. 9).

Basinal sedimentary rocks are intruded by Paleocene to Eocene calc-alkaline and alkaline magmatic rocks. The Sivas, Hekimhan, Malatya, Ulukisla and Central Kizilirmak basins are good examples for these extensional basins in eastern-central Anatolia (Gurer & Aldanmaz 2002; Yılmaz & Yılmaz 2006; Kaymakci *et al.* 2006). These basins formed on top of either ophiolite or ophiolite mélange nappes or a composite basement of ophiolite and rocks of the Tauride–Anatolide Platform, following the terminal closure of the Vardar and Neo-Tethyan Oceans. The Late Cretaceous to Early Cenozoic basins are filled by basal, terrestrial and shallow marine deposits succeeded by deeper turbiditic sequences of Paleocene to Eocene age. Local basin margin thrust faults emplace ophiolite fragments into the sedimentary basin during sedimentation (e.g. Haymana, Çankırı, Sivas and Hınıs). Shallow marine,

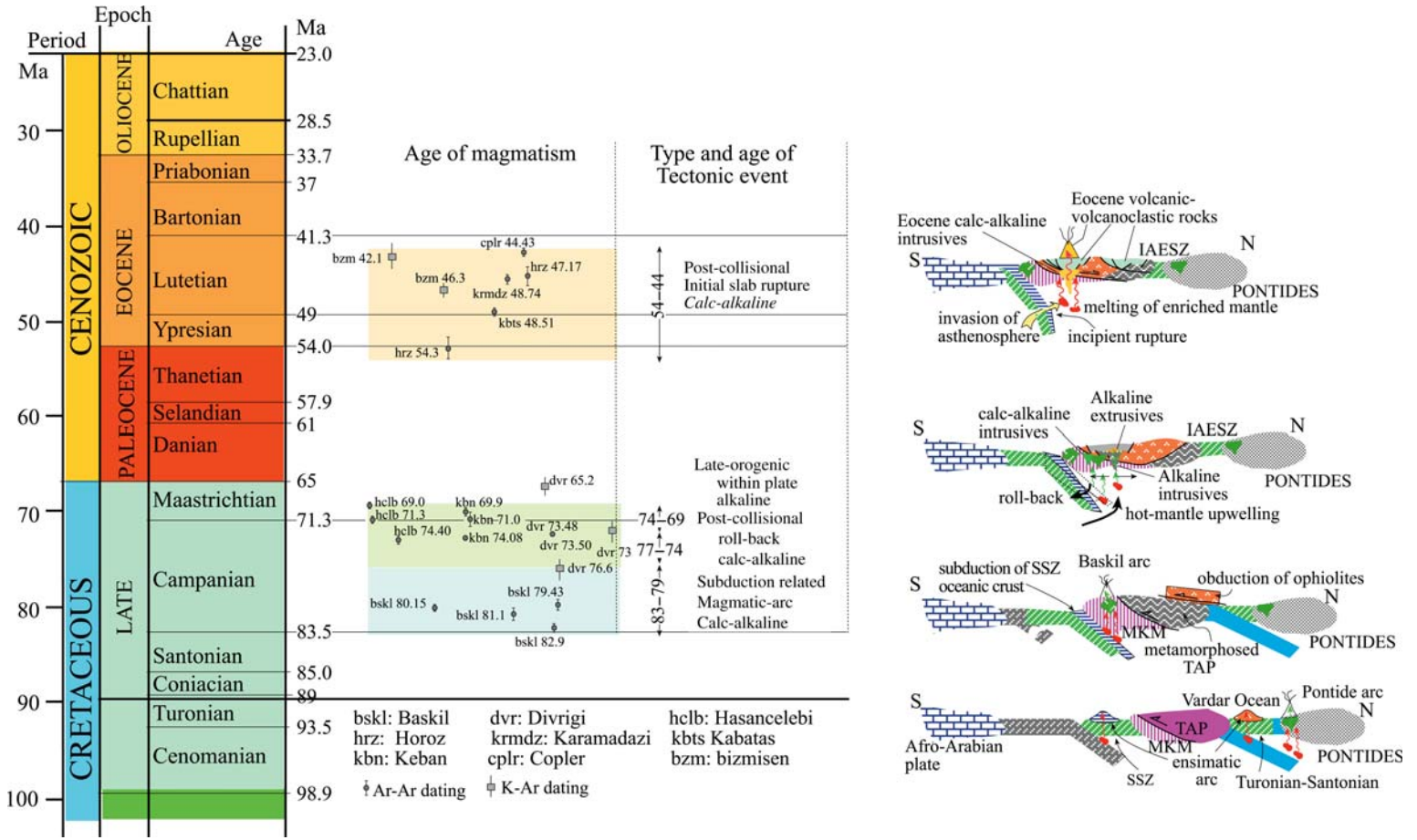


**Fig. 9.** Schematic diagram illustrating the spatial and temporal evolution of magmatism in Baskil-Divrigi transect (error bars represent uncertainties at $\pm 2\sigma$).

marine–deltaic, fluvial–lacustrine and deltaic–lacustrine deposits filled the basin during the Oligocene to Miocene. Alkaline and calc-alkaline, syn- to post-collisional volcanic products intercalated with the basin in-fills during various stages of basin development. For example, syenitic rocks in Hasancelebi intrude latest Cretaceous to Paleocene sedimentary and volcaniclastic infill of the Hekimhan basin. These may indicate that the extension (probably due to roll-back of the subducted slab of the Neo-Tethyan Ocean) reached its maximum creating relatively deep basins and transgression by marine onlap, then, the incipient rupture of the slab may possibly have resulted in invasion of hot asthenospheric mantle through the slab-window towards shallow and low pressure levels in the lithosphere, and partial melting in the mantle. These melts, then, are either emplaced into the marine basins as sill or dykes and volcanic volcano-sedimentary sequences, or as intrusive stocks.

The Arabian/Indian and African continents collided with Eurasian continent along the Bitlis–Zagros in the eastern-southeastern Turkey leading to a thickening crust which underwent incipient slab rupture of the downgoing oceanic plate. Collision appears to have been accompanied by large-scale postorogenic crustal-scale strike–slip faulting and bimodal volcanism during the Early to Middle Eocene. Cessation of subduction likely led to a density increase in the downgoing slab and consequent sinking into the mantle, possibly leading to an initial slab-tear or incipient rupture, leading to the invasion of hot asthenospheric mantle into the overlying mantle wedge (Fig. 9). Although some studies suggest a slab break in eastern and southeastern Anatolia during Late Cretaceous (Boztug *et al.* 2005; Parlak *et al.* 2006) and Eocene (Onal *et al.* 2005), mantle tomography apparently preclude slab break-off at this time in SEAOB and eastern Anatolia. Instead, slab-break or delamination appears to have taken place during mid-Miocene (Sengör *et al.* 2003; Faccenna *et al.* 2006; Hafkenscheid *et al.* 2006; Angus *et al.* 2006) producing wide spread continental volcanism in eastern Turkey (Keskin 2003). It is therefore proposed that post-collisional Eocene magmatic rocks in Copler, Kabatas, Karamadazi and Horoz, which are localized along crustal scale strike–slip faulting, were triggered by an initial rupture in the subducting slab, or by orogenic collapse following the suturing of Afro-Arabian and Eurasian plates (Arabian platform and Anatolides, *sensu stricto*). In each case, hot asthenopheric material moved up into the lower lithosphere, leading to magma generation.

Crucial to the sequence of events proposed herein is the timing of slab break-off in response to the Cenozoic continental collisions between Arabia and Eurasia. Constraints on this event can be obtained by relative convergence velocity. According to Van de Zedde & Wortel (2001), convergence velocities of about 3 cm $a^{-1}$ as in the Arabian region are likely to cause subducting slabs to break off about 10 Ma after the onset of continental collision and subduction of continental lithosphere. The timing of continental collision in Turkey suggests that the subducting slabs should have broken off at around 12 Ma (Hafkenscheid *et al.* 2006). Although this time of slab break-off agrees with other studies (Kohn & Parkinson 2002; Keskin 2003; Sengör *et al.* 2003; Faccenna *et al.* 2006; Hafkenscheid *et al.* 2006; Angus *et al.* 2006), a lower convergence velocity in Arabian plate would have led to a younger break off locally (Van de Zedde & Worte 2001). If continental collision began at about 22 Ma in the Arabian region, Van de Zedde & Wortel (2001) proposed that the slab would have broken off around 12 Ma. They propose an initiation of slab break-off around 30 Ma in the central Arabian region, below the northern Zagros suture zone after which the tear in the slab may have propagated both eastward and westward along the suture zone. This would have led to slab break off around the expected 12 Ma underneath eastern Turkey, as well as below southern Iran.

Considering that the granitoids in the Horoz, Karamadazi, Bizmisen-Calti, Copler and Kabatas regions formed in a post-collisional extension environment between 54.4 and 44.4 Ma, it seems possible that their formation and emplacement does not relate to a slab break off or a subduction, but might relate to the initiation of rupture in the subducting slab (Fig. 9). Upwelling of hot asthenospheric mantle into the incipient rupture would have assisted partial melting in a metasomatized mantle previously contaminated by subduction. Magmas having subduction and/or arc signatures would have resulted.

## Conclusion

Late Cretaceous to Middle Eocene calc-alkaline to alkaline magmatic rocks emplaced within the southeastern Anatolian orogenic belt result from the complex collision between the Afro-Arabian and Eurasian plates and the subduction of the southern and northern Neo-Tethyan oceanic basins beneath the Eurasian continental margin during the Alpine–Himalayan orogeny. During the subduction, the southern branch of Neo-Tethyan Ocean was consumed, and oceanic basin was subducted beneath the eastern Taurides (Eastern Anatolide–Tauride platform) along the Bitlis–Zagros subduction system. Successive collisional and post-collisional events due to slab roll-back and a possible incipient slab rupture played an important role in the magma generation, leading to distinct chemical

compositions ranging from syenite, syenodiorite, trachyte, monzonite, phonolite, granodiorite, diorite, monzodiorite and gabbro. The progression of calc-alkaline to alkaline magmatism within the transect is explained as a consequence of gradual change in the geometry of subduction and slab roll-back followed by a possible incipient slab rupture following the subduction and collision. This led to block faulting and subsidence, and thus to the preservation of near-surface magmatic systems. These vary in time, spatial distribution, and composition. $^{40}Ar/^{39}Ar$ ages supplemented by a few U–Pb ages geochronology from major plutons demonstrate a general younging of magmatism in the transect from *c*. 83 Ma in the south (Baskil) to *c*. 69 Ma in the north (Divrigi-Keban), followed by a *c*. 44 Ma scattered magmatic complexes now found along a NE-trending arcuate belt between Copler and Horoz. The geochemistry in the magmatic rocks suggest two main sources for the melts: (1) a mantle-wedge and subducted oceanic lithosphere producing arc-type magma, and (2) metasomatized lithospheric mantle modified by subduction producing magmatic rocks with more metasomatized mantle and within plate signatures.

The combination of geochemical and geochronological data suggest a temporal and spatial transition from subduction-related to post-collision and to late-orogenic magmatism in the eastern–southeastern Turkey; subduction-related magmatism by the closure of the Neo-Tethyan Ocean whereas post-collision and late orogenic-within plate-related magmatism by the collision of a northern promontory of the SE Anatolian orogenic belt with northerly derived ophiolitic rocks.

The work presented here is part of an on-going research project carried out by the authors at the Mineral Deposits Research Unit at UBC, Canada. The work is generously sponsored by TeckCominco Ltd, Barrick Gold Corp., and Tuprag Metal Madencilik Ltd. The geochemical and geochronological data from Hasancelebi region is part of a research project sponsored by Scientific and Research Council of Turkey (TUBITAK)-CAYDAG with grant no: 103Y023. The authors express their sincere thanks to support from TUBITAK. This paper benefited from reviews by E. Aldanmaz and B. Davies.

## References

Aktas, G. & Robertson, A. H. F. 1984. The Maden Complex, SE Turkey: evolution of a Neotethyan continental margin. *In*: Dixon, J. E. & Robertson, A. H. F. (eds) *The Geological Evolution of the Eastern Mediterranean*. Geological Society, London, Special Publications, **17**, 375–402.

Angus, D. A., Wilson, D. C., Sandvol, E. & Ni, J. F. 2006. Lithospheric structure of the Arabian and Eurasian collision zone in eastern Turkey from *S*-wave receiver functions. *Geophysical Journal International*, **166**, 1335–1346.

Batchelor, R. A. & Bowden, P. 1985. Petrogenetic interpretation of granitoid rocks series using multicationic parameters. *Chemical Geology*, **48**, 43–55.

Beyarslan, M. & Bingol, A. F. 2000. Petrology of a supra-subduction zone ophiolite (Elazig-Turkey). *Canadian Journal of Earth Sciences*, **37**, 1411–1424.

Bird, P. 1978. Finite element modeling of lithosphere deformation: the Zagros collision orogeny. *Tectonophysics*, **50**, 307–336.

Bird, P. 1979. Continental delamination and the Colorado plateau. *Journal of Geophysical Research*, **84**, 7561–7571.

Blevin, P. L. & Chappell, B. W. 1992. The role of magma sources, oxidation states and fractionation in determining the granite metallogeny of eastern Australia. *Transactions of Royal Society Edinburgh*, **83**, 305–316.

Boztuğ, D., Harlavan, Y., Arehart, G. B. & Avci, N. 2005. K–Ar age, whole-rock and isotope geochemistry of A-type granitoids in the Divriği–Sivas region, eastern-central Anatolia, Turkey. *Lithos*, doi: 10.1016/j.lithos.2006.12.014.

Dewey, J. F., Hempton, M. R., Kidd, W. S. F., Saroglu, F. & Sengör, A. M. C. 1986. Shortening of continental lithosphere: the neotectonics of Eastern Anatolia – a young collision zone. *In*: Coward, A. C. & Ries, M. P. (eds) *Collision Tectonics*. Geological Society, London, Special Publications, **19**, 3–36.

Davies, J. H. & Blanckenburg, F. V. 1995. Slab breakoff: a model of lithosphere detachment and its test in the magmatism and deformation of collisional orogens. *Earth and Planetary Science Letters*, **129**, 85–102.

Duggen, S., Hoernle, K., Van Den Bogaard, P. & Garbe-Schonberg, D. 2005. Post-collisional transition from subduction to intraplate-type magmatism in the westernmost Mediterranean: evidence for continental-edge delamination of subcontinental lithosphere. *Journal of Petrology*, **46**, 1155–1201.

Duggen, S., Hoernle, K., Van Den Bogaard, P., Rupke, L. & Phipps Morgan, J. 2003. Deep roots of the Messinian salinity crisis. *Nature*, **422**, 602–606.

Eby, G. N. 1992. Chemical subdivision of the A-type granitoids: petrogenetic and tectonic implications. *Geology*, **20**, 641–644.

Erdem, E. 1994. *Pütürge (Malatya) Metamorfitleri'nin petrografik ve petrolojik ozellikleri*. PhD thesis, Firat University, Turkey.

Faccenna, G., Bellier, O., Martinod, J., Piromallo, C. & Regard, V. 2006. Slab detachment beneath eastern Anatolia: a possible cause for the formation of the North Anatolian fault. *Earth and Planetary Science Letters*, **242**, 85–97.

Fitton, J. G., James, D., Kempton, P. D., Ormerod, D. S. & Leeman, W. P. 1988. Role of lithospheric mantle in the generation of Late Cenozoic basic magmas in the western U.S. *In*: Menzies, M. A. & Cox, K. G. (eds) Oceanic and continental lithosphere: Similarities and differences, *Journal of Petrology Special Volume*, 331–349.

Ghasemi, A. & Talbot, C. J. 2005. A new tectonic scenario for the Sanandaj–Sirjan Zone (Iran).

*Journal of Asian Earth Sciences*, doi: 10.1016/j.jseaes.2005.01.003.

GENC, S. C., YIGITBAS, E. & YILMAZ, Y. 1993. Berit metaofiyolitinin jeolojisi. *In*: KAZANCI, N. (ed.) *Proceedings of Suat Erk Geology Symposium.* Ankara University Geology Department, Ankara, 37–52.

GILL, J. B. 1981. *Orogenic Andesites and Plate Tectonics*. Springer-Verlag, Berlin.

GOVERS, R. & WORTEL, M. J. R. 2005. Lithosphere tearing at STEP faults: response to edges of subduction zones. *Earth and Planetary Science Letters*, **236**, 505–523.

GURER, O. F. & ALDANMAZ, E. 2002. Origin of the Upper Cretaceous–Tertiary sedimentary basins within the Tauride–Anatolide platform in Turkey. *Geological Magazine*, **139**, 191–197.

HAFKENSCHEID, E., WORTEL, M. J. R. & SPAKMAN, M. 2006. Subduction history of the Tethyan region derived from seismic tomography and tectonic reconstructions. *Journal of Geophysical Research*, **111**, B08401, doi: 10.1029/2005JB003791.

HALL, R. 1976. Ophiolite emplacement and the evolution of the Taurus suture zone, south-east Turkey. *Geological Society of America, Bulletin*, **87**, 1078–1088.

HARRIS, N. B. W., PEARCE, J. A. & TINDLE, A. G. 1986. Geochemical characteristics of collision-zone magmatiim. *In*: COWARD, M. P. & RIES, A. C. (eds) *Collision Tectonics.* Geological Society, London, Special Publications, **19**, 67–82.

HAWKESWORTH, C. J., GALLAGHER, K., HERGT, J. M. & MCDERMOTT, F. 1993. Mantle and slab contributions in arc magmas. *Annual Review of Earth and Planetary Sciences*, **21**, 175–204.

HELVACI, C. & GRIFFIN, W. L. 1984. Rb-Sr geochronology of the Bitlis Massif, Avnik (Bingöl) area, S.E. Turkey. *In*: DIXON, J. E. & ROBERTSON, A. H. F. (eds) *The Geological Evolution of the Eastern Mediterranean*. Geological Society, London, Special Publications, **17**, 403–414.

ILBEYLI, N. 2005. Mineralogical–geochemical constraints on intrusives in central Anatolia, Turkey: tectonomagmatic evolution and characteristics of mantle source. *Geological Magazine*, **142**, 187–207.

INNOCENTI, F., MAZZUOLI, R., PASQUARE, G., RADICATI DI BROZOLO, F. & VILLARI, L. 1982. Tertiary and Quaternary volcanism of the Erzurum–Kars area (Eastern Turkey): geochronological data and geodynamic evolution. *Journal of Volcanology and Geothermal Research*, **13**, 223–240.

IRVINE, T. N. & BARAGAR, W. R. A. 1971. A guide to the chemical classification of the common volcanic rocks. *Canadian Journal of Earth Sciences*, **8**, 523–548.

KAYMAKCI, N., INCEOZ, M. & ERTEPINAR, P. 2006. 3D-architecture and Neogene evolution of the Malatya Basin: inferences for the kinematics of the Malatya and Ovacik fault zones. *Turkish Journal of Earth Sciences*, **15**, 123–154.

KELLER, J. 1982. Mediterranean island arcs. *In*: THORPE, R. S. (ed.) *Andesites: Orogenic Andesites and Related Rocks.* John Wiley, Chichester.

KESKIN, M. 2003. Magma generation by slab steepening and break off beneath a subduction-accretion complex: An alternative model for collision-related volcanism in eastern Anatolia, Turkey, *Geophysical Research Letters*, **30**, 8046, doi: 10.1029/2003GL018019.

KOHN, M. J. & PARKINSON, C. D. 2002. Petrologic case for Eocene slab break-off during the Indo-Asian collision. *Geology*, **30**, 591–594.

KUSCU, I., YILMAZER, E. & DEMIRELA, G. 2002. A new 'Fe-oxide-Cu-Au Olympic Dam type' approach to ironoxide deposits in Sivas-Divrigi region. *Geological Bulletin of Turkey*, **45**, 33–46 (in Turkish with English abstract).

KUSCU, İ., GENÇALIOĞLU-KUSCU, G. & TOSDAL, R. M. 2007. Tectonomagmatic-metallogenic framework of mineralization events in the southern NeoTethyan arc, southeastern Turkey. *In*: ANDREW, C. J. (ed.) *Proceedings of 9th Biennial SGA Meeting, Mineral Exploration and Research: Digging Deeper*, Dublin, 1347–1350.

LEAT, P. T., JACKSON, S. E., THORPE, R. S. & STILLMAN, C. J. 1986. Geochemistry of bimodal basalt-subalkaline/peralkaline rhyolite provinces within the southern British Caledonides. *Journal of the Geological Society, London*, **143**, 259–273.

LOPEZ-RUIZ, J., CEBRIA, J. M. & DOBLAS, M. 2002. Cenozoic magmatism I: The Iberian Peninsula. *In*: GIBBONS, W. & MORENO, M. T. (eds) *The Geology of Spain.* Geological Society, London, 417–438.

MAGGIE, A. & PRIESTLY, K. 2005. Surface waveform tomography of the Turkish-Iranian plateau. *Geophysical Journal International*, **160**, 1068–1080.

MANIAR, P. D. & PICCOLI, P. M. 1989. Tectonic discrimination of granitoids. *Geological Society of America Bulletin*, **101**, 635–643.

MCQUARRIE, N., STOCK, J. M., VERDEL, C. & WERNICKE, B. P. 2003. Cenozoic evolution of Neotethys and implications for the causes of plate motions. *Geophysical Research Letters*, **30**, 2036, doi: 10.1029/2003GL017992.

MICHARD, A., WHITECHURCH, H., RICOU, L. E., MONTIGNY, R. & YAZGAN, E. 1984. Tauric subduction (Malatya–Elazig provinces) and its bearing on tectonics of the Tethyan realm in Turkey. *In*: DIXON, J. E. & ROBERTSON, A. H. F. (eds) *The Geological Evolution of the Eastern Mediterranean.* Geological Society, London, Special Publications, **17**, 361–373.

MOIX, P., BECCALETTO, L., KOZUR, H. W., HOCHARD, C., ROSSELET, F. & STAMPFLI, G. M. 2008. A new classification of the Turkish terranes and sutures and its implication for the paleotectonic history of the region. *Tectonophysics*, **451**, 7–39.

NAKAMURA, N. 1974. Determination of REE, Ba, Fe, Na and K on carbonaceous and ordinary chondrites. *Geochimica et Cosmochimica Acta*, **38**, 757–775.

NEUBAUER, F., LIPS, A., KOUZMANOV, K., LEXA, J. & IVAZCANU, P. 2005. Subduction, slab detachment and mineralization in the Neogene in the Apuseni Mountains and Carpathians. *Ore Geology Reviews*, **27**, 13–44.

ONAL, A., BOZTUG, D., KURUM, S., HARLAVAN, Y., AREHART, G. & ARSLAN, M. 2005. K-Ar age determination, whole-rock and oxygen isotope geochemistry of the post-collisional Bizmisen and Calti plutons, SW Erzincan, eastern Central Anatolia, Turkey. *Geological Journal*, **40**, 457–476.

OZGUL, N., TURKUCA, A., OZYARDIMCI, N., BINGOL, I., SENOL, M. & UYSAL, S. 1981. *Munzurların Temel Jeoloji Ozellikleri*. MTA Report **6995**.

PARLAK, O. 2005. Geodynamic significance of granitoid magmatism in the southeast Anatolian orogen: geochemical and geochronogical evidence from Goksun–Afsin (Kahramanmaras, Turkey) region. *International Journal of Earth Sciences*, doi: 10.1007/s00531-005-0058-2.

PARLAK, O., KOZLU, H., DELALOYE, M. & HOCK, V. 2001. Tectonic setting of the Yuksekova ophiolite and its relation to the Baskil magmatic are within the southeast Anatolian orogeny. *In*: *Fourth International Turkish Geology Symposium (ITGS-IV)*, 24–28 September 2001, Adana, Turkey.

PARLAK, O., HOCK, V., KOZLU, H. & DELALOYE, M. 2004. Oceanic crust generation in an island arc tectonic setting, SE Anatolian orogenic belt (Turkey). *Geological Magazine*, **141**, 583–603.

PARLAK, O., YILMAZ, H. & BOZTUG, D. 2006. Origin and tectonic significance of the metamorphic sole and isolated dykes of the Divrigi ophiolite (Sivas, Turkey): evidence for slab break-off prior to ophiolite emplacement. *Turkish Journal of Earth Sciences*, **15**, 25–45.

PEACOCK, M. A. 1931. Classification of igneous rock series. *Journal of Geology*, **39**, 54–67.

PEARCE, J. A. 1983. Role of subcontinental lithosphere in magma genesis at active continental margins. *In*: HAWKESWORTH, C. J. & NORRY, M. J. (eds) *Continental Basalts and Mantle Xenoliths.* Shiva, Nantwich, 230–249.

PEARCE, J. A. 1996. A user's guide to basalt discrimination diagrams. *In*: WYMAN, D. A. (ed.) *Trace Element Geochemistry of Volcanic Rocks: Applications for Massive Sulphide Exploration*. Geological Association of Canada, Short Course Notes, **12**, 79–113.

PEARCE, J. A., HARRIS, N. B. W. & TINDLE, A. G. 1984. Trace element discrimination diagrams for the tectonic interpretation of granitic rocks. *Journal of Petrology*, **25**, 956–983.

PEARCE, J. A. & PEATE, D. W. 1995. Tectonic implications of the composition of volcanic arc magmas. *Annual Review of Earth and Planetary Sciences*, **23**, 251–285.

PEARCE, J. A., BENDER, J. F. *ET AL.* 1990. Genesis of collision volcanism in Eastern Anatolia, Turkey. *Journal of Volcanology and Geothermal Research*, **44**, 189–229.

PERINCEK, D. & KOZLU, H. 1984. Stratigraphical and structural relations of the units in the Afsin-Elbistan-Doganshehir region (Eastern Taurus). *In*: TEKELI, O. & GONCUOGLU, M. C. (eds) *Geology of the Taurus Belt. Proceedings of International Symposium. MTA, Ankara*, 181–198.

PLATT, J. P. & ENGLAND, P. C. 1993. Convective removal of lithosphere beneath mountain belts: thermal and mechanical consequences. *American Journal of Science*, **293**, 307–336.

RICHARDS, J. P. 2003. Metallogeny of the Neo-Tethys arc in central Iran. *In*: ELIOPOULOS, D. G. *ET AL.* (eds) *Proceedings of Mineral Exploration and Sustainable Development.* Millpress, Rotterdam, 1237–1239.

ROBERTSON, A. H. F. 1998. Mesozoic–Cenozoic tectonic evolution of the easternmost Mediterranean area: integration of marine and land evidence. *In*: ROBERTSON, A. H. F., EMEIS, K.-C. & CAMERLENGHI, A. (eds) *Proceedings of the Ocean Drilling Program*. Scientific Results, 723–782.

ROBERTSON, A. H. F. 2000. Mesozoic–Cenozoic tectonic-sedimentary evolution of a south Tethyan oceanic basin and its margins in southern Turkey. *In*: BOZKURT, E., WINCHESTER, J. A. & PIPER, J. D. A. (eds) *Tectonics and Magmatism in Turkey and the Surrounding Area*. Geological Society, London, Special Publications, **173**, 97–138.

ROBERTSON, A. H. F. 2002. Overview of the genesis and emplacement of Mesozoic ophiolites in the Eastern Mediterranean Tethyan region. *Lithos*, **65**, 1–67.

ROBERTSON, A. H. F. & WOODCOCK, N. H. 1982. Sedimentary history of the south-western segment of the Mesozoic–Cenozoic Antalya continental margin, south-western Turkey. *Eclogae Geologicae Helvetiae*, **75**, 517–562.

ROBERTSON, A. H. F. & DIXON, J. E. 1984. Introduction: aspects of the geological evolution of the eastern Mediterranean. *In*: DIXON, J. E. & ROBERTSON, A. H. F. (eds) *The Geological Evolution of the Eastern Mediterranean.* Geological Society, London, Special Publications, **17**, 1–74.

ROBERTSON, A. H. F., USTAOMER, T., PARLAK, O., UNLUGENC, U. C., TASLI, K. & INAN, N. 2005. Late Cretaceous–Early Tertiary tectonic evolution of south-Neotethys in SE Turkey: evidence from the Tauride thrust belt in SE Turkey (Binboga-Engizek segment). *Journal of Asian Earth Sciences*, doi: 10.1016/j.jseaes.2005.02.004.

SAUNDERS, A. D., TARNEY, J. & WEAVER, S. D. 1980. Transverse variations across the Antarctic Peninsula: implications for the genesis of calc-alkaline magmas. *Earth and Planetary Science Letters*, **46**, 344–360.

SAUNDERS, A. D., NORRY, M. J. & TARNEY, J. 1988. Origin of MORB and chemically-depleted mantle reservoirs: Trace element constraints. *In*: MENZIES, M. A. & COX, K. G. (eds) Oceanic and Continental Lithosphere: Similarities and Differences, *Journal of Petrology, Lithosphere Special Issue*, 415–455.

SENGÖR, A. M. C. & YILMAZ, Y. 1981. Tethyan evolution of Turkey: a plate tectonic approach. *Tectonophysics*, **75**, 181–241.

SENGÖR, A. M. C., OZEREN, S., GENÇ, T. & ZOR, E. 2003. East Anatolian high plateau as a mantle-supported, northsouth shortened domal structure. *Geophysical Research Letters*, **30**, 8045, doi: 10.1029/2003GL017858, 2003.

SERRI, G., INNOCENTI, F. & MANETTI, P. 1993. Geochemical and petrological evidence of the subduction of delaminated Adriatic continental lithosphere in the genesis of the Neogene–Quaternary magmatism of central Italy. *Tectonophysics*, **223**, 117–147.

STAMPFLI, G. M. 2001. Tethyan oceans. *In*: BOZKURT, E., WINCHESTER, J. A. & PIPER, J. D. A. (eds) *Tectonics and Magmatism in Turkey and the Surrounding Area*. Geological Society, London, Special Publications, **173**, 1–23.

STAMPFLI, G. M., BOREL, G., MARCHANT, R. & MOSAR, J. 2002. Western Alps geological constraints on western Tethyan reconstructions. *Journal Virtual Explorer*, **8**, 77–106.

TURNER, S. P., PLATT, J. P., GEORGE, R. M. M., KELLEY, S. P., PEARSON, D. G. & NOWELL, G. M. 1999.

Magmatism associated with orogenic collapse of the Betic–Alboran Domain, SE Spain. *Journal of Petrology*, **40**, 1011–1036.

Turner, S., Arnaud, N. *et al.* 1996. Post-collision, shoshonitic volcanism on the Tibetan Plateau: implications for convective thinning of the lithosphere and the source of ocean island basalts. *Journal of Petrology*, **37**, 45–71.

Van De Zedde, D. M. A. & Wortel, M. J. R. 2001. Shallow slab detachment as a transient source of heat at midlithospheric depths. *Tectonics*, **20**, 868–882.

Von Quadt, A., Moritz, R., Peytcheva, I. & Heinrich, C. A. 2005. Geochronology and geodynamics of Late Cretaceous magmatism and Cu–Au mineralization in the Panagyurishte region of the Apuseni–Banat–Timok–Srednogorie belt, Bulgaria. *Ore Geology Reviews*, **27**, 95–126.

Wilson, M. 1989. *Igneous Petrogenesis*. Kluwer, Dordrecht.

Wilson, M. & Bianchini, G. 1999. Tertiary–Quaternary magmatism within the Mediterranean and surrounding regions. *In*: Durand, B., Jolivet, L., Horvath, F. & Serrane, M. (eds) *The Mediterranean Basins: Tertiary Extension within the Alpine Orogen*. Geological Society, London, Special Publications, **156**, 141–168.

Winchester, J. A. & Floyd, P. A. 1977. Geochemical discrimination of different magma series and their differentiation products using immobile elements. *Chemical Geology*, **20**, 325–343.

Wortel, M. J. R. & Spakman, W. 2000. Subduction and slab detachment in the Mediterranean–Carpathian region. *Science*, **290**, 1910–1917.

Yazgan, E. 1984. Geodynamic evolution of the eastern Taurus region. *In*: Tekeli, O. & Göncüoglu, M. C. (eds) *Proceedings of Geology of the Taurus Belt*. MTA, Ankara, 199–208.

Yazgan, E. & Chessex, R. 1991. Geology and tectonic evolution of the Southeastern Taurus in the region of Malatya. *Turkish Association of Petroleum Geologists Bulletin*, **3**, 1–42.

Yigitbas, E. & Yilmaz, Y. 1996. New evidence and solution to the Maden complex controversy of the southeast Anatolian orogenic belt (Turkey). *Geologische Rundschau*, **85**, 250–263.

Yilmaz, Y. 1993. New evidence and model on the evolution of the southeast Anatolian orogen. *Geological Society of America Bulletin*, **105**, 251–271.

Yilmaz, Y., Yigitbas, E. & Yildirim, M. 1987. Güneydogu Anadolu'da Triyas sonu tektonizmasi ve bunun jeolojik anlami. *Proceedings of the Turkish 7th Petroleum Congress*, 65–77.

Yilmaz, Y., Yigitbas, E. & Genç, S. C. 1993. Ophiolitic and metamorphic assemblages of Southeast Anatolia and their significance in the geological evolution of the orogenic belt. *Tectonics*, **12**, 1280–1297.

Yilmaz, A. & Yilmaz, H. 2006. Characteristic features and structural evolution of a post-collisional basin: the Sivas Basin, Central Anatolia, Turkey. *Journal of Asian Earth Sciences*, **27**, 164–176.